THE JOURNAL OF COMPARATIVE NEUROLOGY 365:659–682 (1996)

Laminar and Columnar Patterns of Geniculocortical Projections in the Cat: Relationship to Cytochrome Oxidase

JAMIE D. BOYD AND JOANNE A. MATSUBARA
Departments of Ophthalmology (J.D.B., J.A.M.) and Anatomy (J.A.M.),
University of British Columbia, Vancouver, British Columbia, Canada V5Z 3N9

ABSTRACT

We examined the laminar and columnar arrangement of projections from different layers of the lateral geniculate nucleus (LGN) to the visual cortex in the cat. In light of recent reports that cytochrome oxidase blobs (which in primates receive specific geniculate inputs) are also found in the visual cortex of cats, the relationship between cytochrome oxidase staining and geniculate inputs in this species was studied. Injections of wheat germ agglutinin-conjugated horseradish peroxidase were made into the anterior "genu" of the LGN, where isoelevation contours of the geniculate layers are distorted due to the curvature of the nucleus. Consequently, anterograde labeling from the various LGN layers was topographically separated across the surface of the cortex, and labeling in a particular isoelevation representation of the cortex could be associated with a specific layer of the LGN. Labeling from the A layers, which contain X and Y cells, was coextensive with layers 4 and 6 in both area 17 and area 18, as previously reported. Labeling from the C layers, which contain Y and W cells, occupied a zone extending from the 4a/4b border to part way into layer 3 in area 17. The labeling extended throughout layer 4 in area 18. There was also labeling in layer 5a and layer 1 in both area 17 and area 18. Except in layer 1, labeling from the C layers was patchy. In the tangential plane, adjacent sections stained for cytochrome oxidase showed that the patches of labeling from the C laminae aligned with the cytochrome oxidase blobs. The cytochrome blobs were visible in layers 3 and 4a, but not in layer 4b in both areas 17 and 18. These results suggest that W cells project specifically to the layer 3 portion of the blobs, while Y cells, at least those of the C layers, project specifically to the layer 4a portion of the blobs in area 17. The heavy synaptic drive of the Y cells is probably the cause of the elevated metabolism, and thus, higher cytochrome oxidase activity, of the blobs.

Indexing terms: lateral geniculate nucleus, visual cortex, Y-cells, W-cells, processing streams

The lateral geniculate nucleus (LGN) is the main thalamic relay between the retina and the visual cortex. In the cat, three main classes of LGN cells, known as X, Y, and W, have been distinguished on both physiological and anatomical criteria (see Casagrande and Norton, 1991 for review). These separate populations of LGN relay cells each receive input from corresponding classes of retinal ganglion cells (Cleland et al., 1971; Hoffman et al., 1972; Boycott and Wässle, 1974; Leventhal et al., 1985). Thus, three parallel streams of information originate in the retina and are kept separate in the LGN. What is less clear is whether X, Y, and W inputs from the LGN are kept separate in the visual cortex, or at what stage they might be integrated.

Different classes of LGN terminations are only partially segregated into separate layers of the cortex. Thus, in area 17, intracellular fills of single, physiologically characterized LGN afferents have shown that, while Y afferents are mostly confined to the upper half of layer 4, X afferents terminate throughout the depth of this layer. Both X and Y axons make collaterals to layer 6 (Freund et al., 1985; Humphery et al., 1985a,b). In area 18, where X afferents are rare or absent, Y afferents terminate throughout the depth of layer 4, but still appear to terminate most heavily in the upper part of the layer. No W afferents have been intracellularly filled, probably due to their smaller diameter. Bulk injections of tracers in the C laminae of the LGN, which contain both Y and W cells, resulted in labeling at the layer 3/4 and the layer 4/5 borders in area 17 and throughout layer 4 in area 18 (LeVay and Gilbert, 1976). LeVay and Gilbert also noted that the labeling from the C laminae had

Accepted June 21, 1995.

Address reprint requests to Joanne Matsubara, Eye Care Centre, 2550 Willow Street, Vancouver, British Columbia, Canada V5Z 3N9.

a patchy distribution in the cortex, being present in some cortical columns but not others. They speculated that the patches of labeling following C-laminae injections corresponded to ocular dominance columns, although the C-laminae receive inputs from both eyes (Guillery, 1970; Hickey and Guillery, 1974; Guillery and Oberdorfer, 1977).

The laminar pattern of geniculate terminations in visual cortex is thought to be related to that shown by histochemical staining for the metabolic enzyme cytochrome oxidase (CO). It has been repeatedly shown that termination sites of thalamic inputs often have high levels of CO staining, and that levels of CO staining are correlated with levels of neuronal activity (Wong-Riley, 1979; Wong-Riley and Riley, 1983; Wong-Riley et al., 1989). It is thought that the high activity level of geniculate terminals, in turn, creates higher activity levels in cortical cells mono-synaptically activated from the LGN. The higher activity levels in geniculate recipient layers means these layers will have increased metabolic demand and, therefore, higher CO levels relative to cortical layers not receiving direct input from the LGN (Kageyama and Wong-Riley, 1986a).

In all primate species examined, cytochrome oxidase staining mirrors the segregation of geniculocortical terminals not only into particular lamina, but also into particular cortical columns, as cells in the koniocellular layers of primate LGN project to CO blobs, but not to interblobs, in layer 3 of primary visual cortex (Hendrickson et al., 1978; Fitzpatrick et al., 1983, Weber et al., 1983; Horton, 1984; Livingstone and Hubel, 1987b; Lachica and Casagrande, 1992). The densely staining CO blobs and lightly staining interblobs correspond to an elaborate segregation not only of LGN inputs, but also of corticocortical outputs and physiological response properties (Livingstone and Hubel, 1983, 1984, 1987a, 1988). This division of visual cortex into two sets of columns with fundamental differences in organization has only been shown in primates; until recently, it was thought that the CO blob/interblob system was not present in non-primates such as the cat. However, reports of CO blobs in cat and ferret (Murphy et al., 1990; Boyd and Matsubara, 1992; Cresho et al., 1992; Dyck and Cynader, 1993b) raise the possibility that a similar division may exist in non-primates.

It was wondered whether LGN projections in the cat might also show a relationship with CO staining, as has been shown for the koniocellular LGN projection in primates. As the W-cells of the cat bear a certain resemblance to cells in the primate koniocellular layers in their small size, projection outside of layer 4, and physiological responses (Casagrande and Norton, 1991), it was wondered whether the patchiness of W-cell projection to layer 3 in the cat might also be related to CO staining. Such a demonstration would show the cat visual system to possess some of the structural motifs shown in the primate, and would help to explain the significance of the CO blobs in the cat.

In this paper, the terminations of different geniculocortical projections in the cat were examined. These were compared to CO staining patterns to determine which classes of geniculate afferents are correlated with high levels of CO activity and, in particular, which classes of afferents provide input to the CO blobs. A preliminary account of this work has been previously presented (Boyd and Matsubara, 1993).

METHODS

Experiments were performed on eight adult cats of both sexes. Some of these cats were also used for electrophysiological recordings unrelated to the present experiments. We also examined sections through the LGN and cortex from a separate series of experiments in this laboratory involving cortical injections of tracers. These were used to demonstrate the general topography of the geniculocortical projection. Before surgery, animals were given an intramuscular injection of a mixture of 0.5 mg/kg acepromazine maleate (atravet; M.T.C. Pharmaceuticals) and 0.05 mg/kg atropine sulfate (M.T.C. Pharmaceuticals). Animals were also given an intramuscular injection of 0.05 mg/kg dexamethasone (Austin Laboratories) to reduce brain edema. Anesthesia was maintained during surgery by an intravenous injection of sodium methohexital (Brietal; Eli Lilly Canada, Inc.), to effect. The sites of all incisions were injected with 3–5 ml of a long lasting local anesthetic, 0.25% bupivacaine hydrochloride (Marcaine; Winthrop Laboratories). The saphenous vein was cannulated and a tracheotomy was performed. The animal was then positioned in a stereotaxic frame and a craniotomy and duratomy were performed over stereotaxic coordinates AP +4 to +9 and ML 7 to 12 mm. These coordinates, targeting the lower visual field representation, were chosen using Sanderson's map of the LGN (Sanderson, 1971a).

After all surgery was completed, the animal was paralyzed with gallium triethiodide (Rhone-Poulenc Pharma) and artificially respired with a 70:30 mixture of nitrous oxide and oxygen. The animal was infused with 10 mg/kg/hr gallium triethiodide and 1.0 mg/kg/hr sodium pentobarbital dissolved in 5% dextrose in lactated Ringer's solution. The EEG and EKG were monitored and the end-tidal pCO_2 was maintained near 4%. Contact lenses were inserted having 4 mm artificial pupils and the appropriate refractive power to focus the eyes on the tangent screen.

Electrophysiological recording of visual responses was used to place the injection sites within the LGN. Visual stimuli (bright spots 1–10° diameter on a dark background) were generated with a computer driven projector. Signals from glass insulated platinum-iridium electrodes (resistance 0.5–1.0 MΩ) were bandpass-filtered to remove 60 Hz noise, amplified, and displayed on an oscilloscope and an audio monitor. On the basis of eye-specific inputs, the LGN of the cat is divisible into the dorsal A laminae, composed of lamina A (contralaterally driven) and lamina A1 (ipsilaterally driven), and the ventral C laminae, composed of upper, magnocellular lamina C (contralaterally driven), and lower, parvicellular laminae C1 (ipsilateral) and C2 (contralateral; Guillery, 1970; Hickey and Guillery, 1974; Guillery and Oberdorfer, 1977). The layers of the LGN were thus located by following the shifts in eye dominance from contralateral to ipsilateral, and back to contralateral eye, as the electrode traversed the lamina A, A1, and C. It was not possible to record a shift to ipsilateral responses at the C/C1 border, probably because the low impedance of the electrodes precluded recording from the very small cells in layers C1 and C2, or because these cells were not responsive under the anesthetic regime used. Therefore, we began the injections 0.5–1.0 mm below the last recorded visual response.

Injection sites were specifically chosen in areas where receptive field elevation changed rapidly along the penetration (see results). At such sites, the isoelevation projection

lines of the visual field run at steep angles to the coronal plane (Sanderson, 1971b). Therefore, although the injection site usually included layer A1, and even, in some cases, layer A, as well as all of the C laminae of the LGN, labeling from the different laminae was separated topographically in the cortex.

After locating the correct site in the LGN, the metal electrode was replaced with a glass pipette containing 2% wheat germ agglutinin-horseradish peroxidase (WGA-HRP) in saline. Electrical recordings could also be obtained through the glass pipette. Although no single units could be isolated, the background multi-unit "hash" showed clear shifts in eye dominance so that the position of the injection could be verified. When the appropriate injection site was found, polyethylene tubing was attached to the back of the pipette and air pressure from a syringe was used to inject 0.1 to 0.5 μl of tracer.

Twenty-four hours was allowed to pass from the time of the last injection until perfusion. Animals were euthanized with an overdose of barbiturate, then perfused with 1,500 ml phosphate buffer (0.1 M, pH 7.2) with 0.5% sodium nitrite. This was followed by 400 ml of 4% paraformaldehyde in phosphate buffer delivered over 5–7 minutes. In four cases, the cortex was sectioned coronally at 75 μm on a freezing microtome. In the remaining four cases, visual cortex was removed from the brainstem and unfolded and flattened (Olavarria and Van Sluyters, 1985). The flattened cortical blocks were left 16–40 hours in 4% paraformaldehyde and 25% sucrose in phosphate buffer and then sectioned tangentially at 50 μm. In all cases, the thalamus was sectioned coronally at 75 μm to verify injection site placement.

In all cases, one one-in-two series of sections was reacted for WGA-HRP using the standard tetramethylbenzidine (TMB) method (Mesulam, 1978) and counterstained for Nissl substance with neutral red. The alternate series of sections was reacted for cytochrome oxidase using a protocol modified from various authors (Horton and Hubel, 1981; Silverman and Tootell, 1987; Crockett et al., 1993). The reaction solution consisted of 20–25 mg diaminobenzidine, 30 mg cytochrome C, 15 mg catalase, and 1 g sucrose dissolved in 100 ml 0.06 M phosphate buffer pH 7.2, to which was added 3–5 ml of a 1% nickel ammonium sulfate solution and 3–5 ml of a 1% cobalt chloride solution. Free floating sections were incubated for 2–4 hours. Sections were floated onto gelatin coated slides, air-dried overnight, dehydrated in an ascending series of alcohols, cleared in xylene, and then mounted with DPX mounting medium.

Eight bit images of anterograde HRP labeling and CO staining in tangential sections were captured using a Cohu CCD camera (4915) and a Data Translation (DT-2255) frame grabber card with NIH Image v. 1.47 software running on a Macintosh IIfx computer. Using radially oriented blood vessels as landmarks, sections stained for

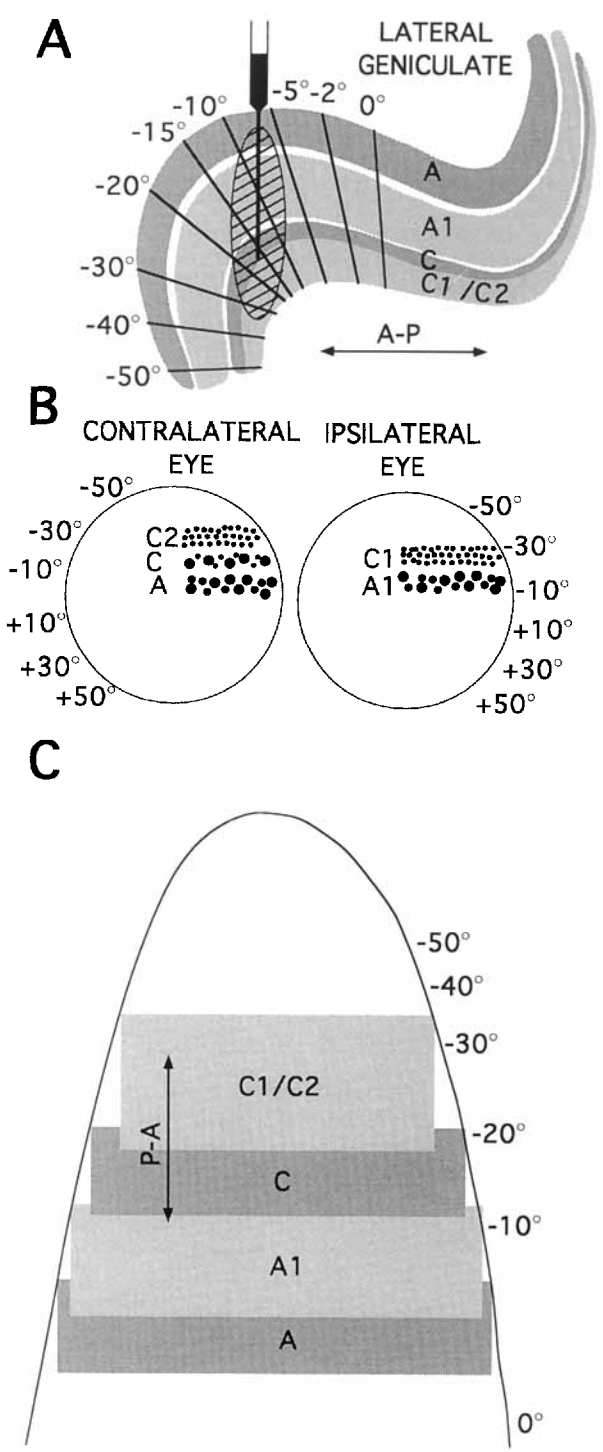

Fig. 1. Schematic diagram of the isoelevation map in the geniculate and how aspects of its organization were utilized to obtain topographically separated labeling from different geniculate laminae. **A:** A parasagittal section of the lateral geniculate with isoelevation lines marked for the lower visual field. An injection pipette in the coronal plane passing through the curved anterior part of the nucleus traverses a wide span of elevation, and each geniculate lamina is injected at a different, though slightly overlapping, range of elevations. Lamina A will be injected at representations of higher elevations, and lamina C1 and C2 at lower elevations. **B:** The expected pattern of labeling in the retinae. A zone of labeling corresponding to each lamina is present, and these zones are separated across the retina. The X, Y, and W cell classes labeled from each geniculate lamina are shown as three different sizes of dots, W-cells being the smallest and Y-cells being the largest. **C:** The expected distribution of labeling in the cortex. In this view of a flattened cortex, the border of the oval-shaped lower visual field representation of area 17 is outlined, and approximate isoelevations for the visual field map are indicated. As in the retina, labeling from the various geniculate layers is segregated according to the elevation representation injected in each geniculate lamina. Thus, labeling from layers C1 and C2 is found further anterior, and labeling from lamina A is found further posterior in area 17.

CO were aligned with adjacent HRP stained sections by an Image module allowing precise superimposition of successive images. Pixel values for each image were saved to a text file. The strength of the relationship between pixel values at corresponding locations in two such aligned images was assessed by linear regression using StatView (Abacus Concepts, Inc.).

RESULTS

We used the technique of injecting multiple geniculate lamina with a single injection, but at varying retinotopic locations. The rationale for this technique is illustrated in Figures 1 and 2. Figure 1 is a schematic diagram showing receptive field isoelevations for an injection site in the LGN and for the resulting labeling in the cortex and retina. As shown in Figure 1A, a vertically oriented pipette penetration into the curved region in the anterior part of the LGN traverses a 30° range of isoelevations. Elevation steadily decreases as the pipette passes from A through A1 and C and into the ventral C laminae. Differing elevation representations are thus injected in each layer. As elevation is also mapped across the surface of the retina (Fig. 1B) and the cortex (Fig. 1C), labeling from the different LGN layers will be separated across the surface of these structures. Retinotopic separation of labeling from different LGN layers following a single LGN injection has been previously noted by Illing and Wässle (Illing and Wässle, 1981). In a study of retinogeniculate projections, they injected the curved region in posterior part of the LGN and found separated sectors of labeling in the contralateral retina.

Figure 2 shows results from tracer injections illustrating the mapping of geniculocortical and retinogeniculate projections as outlined in Figure 1. Figure 2A,B show retrograde labeling in the LGN from the three small, widely separated injections of retrograde tracers in the visual cortex shown in Figure 2C. Figure 2B is at an A-P level where isoelevation lines are nearly parallel to the coronal plane; labeling from a single cortical injection site (the most posterior one) therefore appears throughout all of the geniculate laminae. This is in contrast to the situation in Figure 2A, which shows a section anterior to the one in Figure 2B. At this level, isoelevation projection lines run at steep angles to the coronal plane. Labeling from all three injection sites shown in Figure 2C are present in this one section, thus showing that the representation of elevation changes greatly from lamina A to lamina C2. The section in Figure 2A is at the approximate level where injections were made for this study, an example of which is shown in Figure 2D. This was one of the larger injections used in this study, yet labeling in the cortex from A- and C-geniculate laminae was still segregated anteroposteriorly.

Topographical separation of labeling from the various LGN laminae was also seen in the retina. Labeling in topographically separated parts of the retina could be verified as arising from different layers of the LGN because different LGN laminae receive input from different classes of ganglion cells. The parvicellular division of the C laminae (layers C1 and C2) receive mostly input from W retinal ganglion cells. The magnocellular division of the C laminae (layer C) receives inputs from Y and W retinal ganglion cells, and the A laminae (layers A and A1) receive input from X and Y retinal ganglion cells (Guillery and Oberdorfer, 1977; Guillery et al., 1980; Leventhal, 1982; Leventhal et al., 1985). The fact that different classes of retinal ganglion cells were labeled at different elevations in the retina is evidence that we were successful in injecting different LGN layers at different elevation representations.

Figure 2E shows a low power photomicrograph of the flat-mounted retina ipsilateral to the LGN injection shown in Figure 2D. Lower visual field elevations are shown in the lower part of the figure. With progression from higher into lower representations of visual fields, the pattern of labeling changes such that only smaller retinal ganglion cells are labeled. Higher magnification photomicrographs of the area in the lower part of Figure 2E show large, unlabeled ganglion cells (Fig 2G, arrowheads) intermixed with the smaller, retrogradely labeled cells. Thus, the portion of the injection site which extended into lamina A1 resulted in labeling of many large (X and Y) retinal ganglion cells, and only at higher receptive field elevations. In contrast, the part of the injection site extending into layer C1 resulted in the labeling of only the smaller (W) ganglion cells, and only at lower elevations. In this experiment, a relatively large amount of HRP was used, so that the visual field representations of the different LGN layers injected were relatively large and overlapped somewhat. The injected visual field representation of layer C (which receives input from the contralateral eye) was completely overlapped by the visual field representations injected in surrounding layers A1 and C1. An unlabeled region of ipsilateral retina sandwiched between lower elevations labeled from layer C1 and higher elevations labeled from layer A1 was thus not present.

Cytochrome oxidase staining

As the goal of this study was to compare patterns of geniculocortical labeling to the pattern of CO staining, the laminar and columnar organization of the latter in area 17 and 18 will first be described (see Figs. 3–5). The laminar terminology employed in this study was that of O'Leary (1941), and as further expounded by Lund et al. (1979). Although originally developed for area 17, this laminar scheme has also been used for area 18 (Friedlander and Martin, 1989), and we have done the same. In this scheme, the layer 3/4 border is at the level of the largest pyramidal cells in the upper layers, the so-called "border pyramids." Layer 4 is divided into sublayers 4a and 4b. Layer 4a has many large stellate cells in addition to smaller stellate cells and some pyramidal cells. Layer 4b is composed mostly of small stellates, and is more tightly packed than 4a. In addition, we noted that layer 4b could often be subdivided into upper and lower sublayers based on the fact that the lower portion of layer 4b contained smaller, more closely packed cells than the upper portion. The subdivision of layer 4b was noted in both area 17 and 18 and is visible in Figure 3A. Figure 3A shows the border between areas 17 and 18 in a Nissl stained section, flanked by matched areas in an adjacent section stained for CO. The laminar pattern of CO staining was generally in agreement with previous studies (Wong-Riley, 1979; Kageyama and Wong-Riley, 1986b). In both areas 17 and 18, a dense band of CO staining was coextensive with layer 4 as determined by cytoarchitecture. There was also moderately dense CO staining in layer 3. The border between this moderate level of staining in layer 3 and the dense band of layer 4 was usually quite sharp. In our material, the large pyramids at the layer 3/4 border often stained for CO. Below 4b is layer 5a, a thin layer of very small pyramids. This layer does not stain for CO. Layer 5b contains both large and medium pyramidal cells, and is very loosely packed. The largest

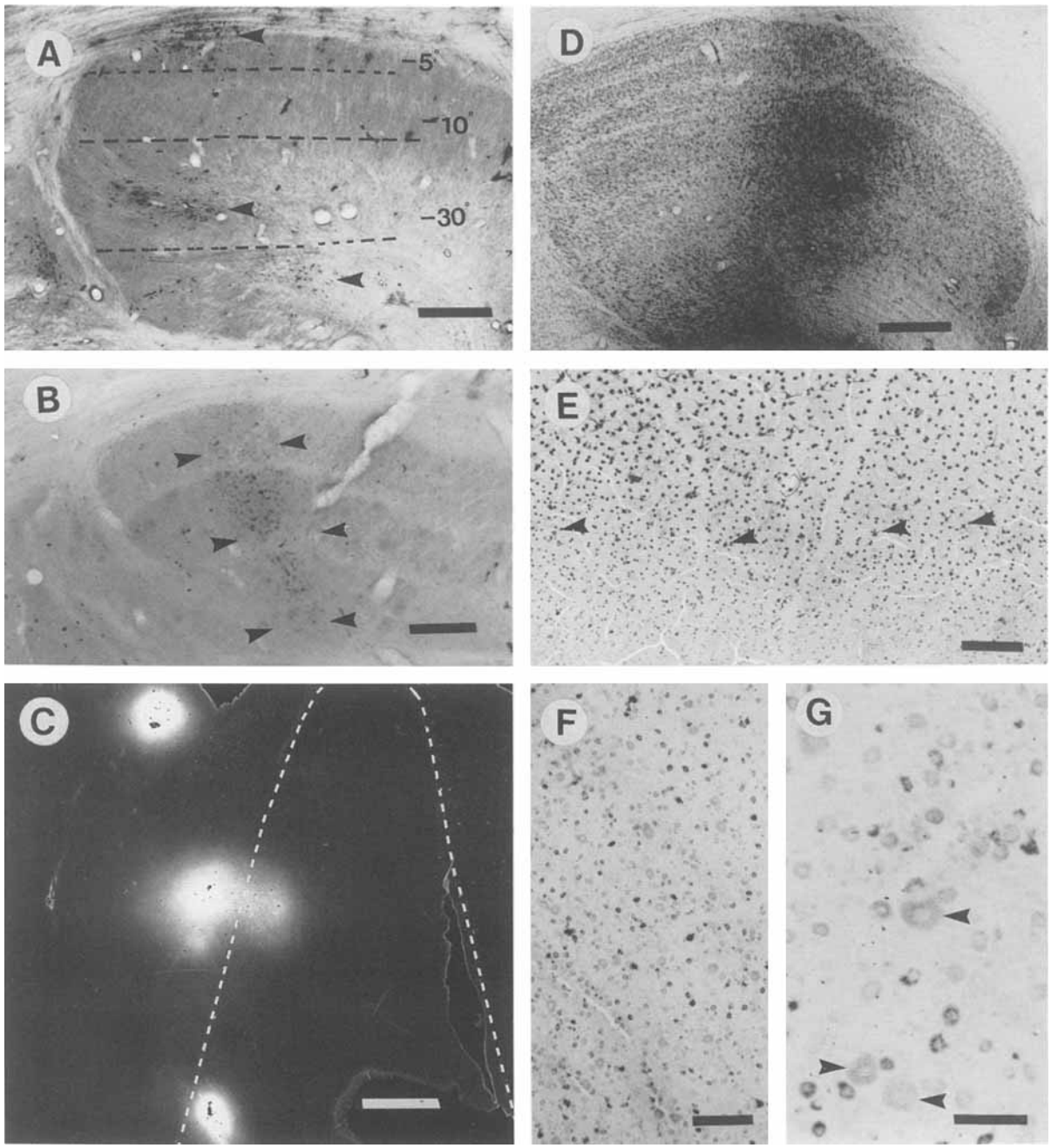

Fig. 2. Results from tracer studies demonstrating the mapping outlined in Figure 1. **A, B:** Coronal sections of the lateral geniculate nucleus (LGN) at anterior-posterior levels +7.5 and +6.0, respectively. Approximate positions of isoelevation lines (Sanderson et al., 1971) are shown (dashed lines) in A; the A-P level of B corresponds roughly to a plane of isoelevation at 0°. Scale bars in A, B, 500 μm. A reverse contrast photograph of a flattened, tangential section of visual cortex from the same animal is shown in **C.** The outline of area 17 is shown in dashed white lines. Scale bar, 2 mm. Three injections of retrograde tracers, widely separated in the A-P dimension (and thus with greatly differing isoelevations) were made into areas 17 and 18 of this animal. A single column of labeling (between arrowheads), arising from only the most posterior injection site and extending across all of the geniculate layers, is present in B, but three separate clusters of labeling in different geniculate layers, each from a different injection site (arrowheads) are found in A. A brightfield photomicrograph of a typical injection of WGA-HRP in the LGN is shown in **D.** The injection is at a similar A-P level as the section shown in A. The injection site included all layers of the LGN. Scale bar, 500 μm. **E:** A photomicrograph of the ipsilateral retina from this experiment, flat-mounted, stained for HRP, and lightly counterstained with neutral red. Lower elevations, corresponding to the part of the parvicellular C laminae injected, are represented at the bottom of the photograph. The arrowheads mark four retrogradely labeled Y ganglion cells, recognized by their large cell bodies and dendritic arborization. Above these cells, many other Y ganglion cells are labeled; below these cells, only small ganglion cells are labeled. Scale bar, 200 μm. **F, G:** The area of small cell labeling at higher magnifications. Large ganglion cells stained with neutral red can be seen, arrowheads in G, but these do not contain HRP reaction product, present in the smaller cells. Scale bar in F, 100 μm. Scale bar in G, 25 μm.

pyramidal cells in area 17, the Meynert cells, are found at the 5a/5b border, and these cells were densely stained for CO (Kageyama and Wong-Riley, 1986a). Often, a thin band of neuropil staining was coextensive with these large pyramids, giving layer 5 a trilaminar appearance, as the rest of layer 5b did not stain for CO. Layer 6 is composed of small and medium sized pyramidal cells, and can be differentiated from layer 5b by its more tightly packed cells. This layer stained moderately for CO.

An identical pattern of CO staining was found in area 18, in disagreement with a previous report that the dense band of CO staining in layer 4 in this area extended part way into layer 3 (Price, 1984). This discrepancy is probably due to a different assignation of the layer 3/4 border, rather than true differences in staining patterns. In particular, the large cells in layer 4a tend to be larger in area 18 than in area 17, as can be seen clearly in Figure 3C. Larger cells, such as these, have apparently been mistaken for "border pyramids" in area 18, resulting in deeper placement of the layer 3/4 border. We also noted that some of the large cells in layer 4a of area 18 were clearly not standard pyramidal cells. One of the cells shown in Figure 3D has a thin apical dendrite as well as other dendrites originating from various positions around the cell soma, giving it the appearance of a star-pyramid, a cell characteristic of layer 4 in area 17.

In addition to the laminar variation of CO staining, there was also a marked columnar organization, i.e., the CO "blobs." Figure 4 shows low power views of the CO blobs in the coronal (Fig. 4A) and tangential (Fig. 4B) planes. The center-to-center spacing of the blobs, uncorrected for shrinkage (estimated to be around 20%), was about 0.75 mm. In the tangential plane, the blobs were not arranged in orderly rows, as was found to be the case in some primates. The area between the solid black lines in Figure 4A is shown at higher power in Figure 4C. The fluctuation in staining density seen in the tangential plan, corresponding to the CO blob/interblob system, is present in the upper part of layer 4 and in layer 3 (Fig. 4C,D). Also, note the neuropil staining surrounding the CO labeled Meynert cells in layer 5, giving this layer a trilaminar appearance, as mentioned above. Figure 4D shows a high power photomicrograph through layer 4. A CO blob to the left of the figure is marked by dense staining in layer 4a, with only moderate staining in 4b. To the right of the figure, in an interblob zone, there is little difference in the staining intensity of layers 4a and 4b. Note that, in addition to neuropil staining, several stained cell bodies are visible. Two large pyramidal cells at the layer 3/4 border are marked with arrowheads. These border pyramids were clearly seen in tangentially cut sections through the layer 3/4 border stained for CO. Several such cells can be seen in Figure 4E embedded in a meshwork of CO reactive processes. These cells can be identified as pyramidal cells by their apical dendrites, which are viewed face-on and thus appear fore-shortened. Basal dendrites can often be seen as well.

The photomicrographs of Figure 5 show nine alternate 50 μm sections progressively deeper into the same zone of cortex in area 17. The first three sections (Fig. 4A–C) are mostly through layer 3. The CO blobs first appear, albeit faintly, in the middle part of this layer, becoming more visible towards the bottom of layer 3, as seen in Figure 5B,C. In Figure 5B,C, CO stained cell bodies can be seen as small dark spots which are more numerous within the CO blobs; these cells are the layer 3/4 border pyramids. Figure 5D,E contains mostly layer 4a, and it is in this layer where the blobs are most visible. Although Figure 5A,B also show layer 4a, these prints were intentionally overexposed to show the faint staining of blobs in layer 3. Consequently, layer 4a in these sections appears densely and evenly stained which was not, in fact, the case. Figure 5F,G contain mostly layer 4b. The blobs are not visible in this layer, and the CO staining has a fine mesh-work pattern to it, which differentiates it from layer 4a. This pattern may result from the tight packing of cells in this layer, which might constrain the positions of reactive dendrites and axon terminals. The darkly stained Meynert cells are clearly visible wherever the layer 5a/5b border is in the plane of section. A large expanse of these cells is visible in Figure 5I. Layer 6, which can first be seen in Figure 4F, was found to be uniformly stained and the CO blobs were not visible in this layer.

Laminar organization of geniculocortical projections

Figures 6–11 present the results of the laminar distribution of geniculocortical projections from different layers of the LGN to cortical areas 17 and 18. As described in the materials and methods, injections were made in such a way that different LGN laminae were injected at different isoelevation representations. As the pipette passed through representations of lower azimuths in the C laminae than in the A laminae, labeling from the C laminae was found more anteriorly in the visual cortex, and labeling from the A laminae was found more posteriorly. The position of coronal sections with respect to both the well established visual field map of areas 17 and 18 (Tusa et al., 1978, 1979), and the overall extent of labeling, was recorded. With this information, it was possible to classify labeling in the cortex as arising from the A laminae versus arising from the C laminae. Labeling from the A laminae of the LGN is shown in Figure 6. Ocular dominance (OD) columns were often visible, as in Figure 6A, showing that labeling arising from a single lamina could be isolated. As this section was just slightly posterior to sections containing labeling from the C laminae, it is assumed that the labeling in Figure 6a arose from lamina A1. (With slightly larger injections, labeling from both layer A and layer A1 could be obtained at some locations in the cortex, and in these cases, labeling in layer 4 was continuous.) Adjacent sections stained for CO showed a band of heavy staining of CO in layers 4 and 6 that perfectly matched the terminal labeling in these layers. Layer 6 contained retrograde as well as anterograde labeling. In some experiments, many of the large cells at the border of layers 5a and 5b were also labeled, possibly due to the spread of the injection into part of the lateral posterior/pulvinar nucleus (Mason, 1978; Lund et al., 1979). Although their labeling in this material was fortuitous, these cells provided a useful guide to the 5a/5b border in the dark-field photographs. The clear gap between these cells and the band of labeling showed that layer 5a was not labeled from the A laminae of the geniculate. Note in Figure 6A the difference in density of projections to upper and lower parts of layer 4 in some of the patches of labeling (shown most clearly by the left-most patch of labeling). Figure 6B and C show darkfield and brightfield views of a single patch of A laminae labeling in layer 4. When compared to the Nissl staining, it is evident that the borders of the labeling from the A laminae match the borders of layer 4. Moreover, the clear boundary between the upper, denser labeling, and the lower, less dense input matches the border

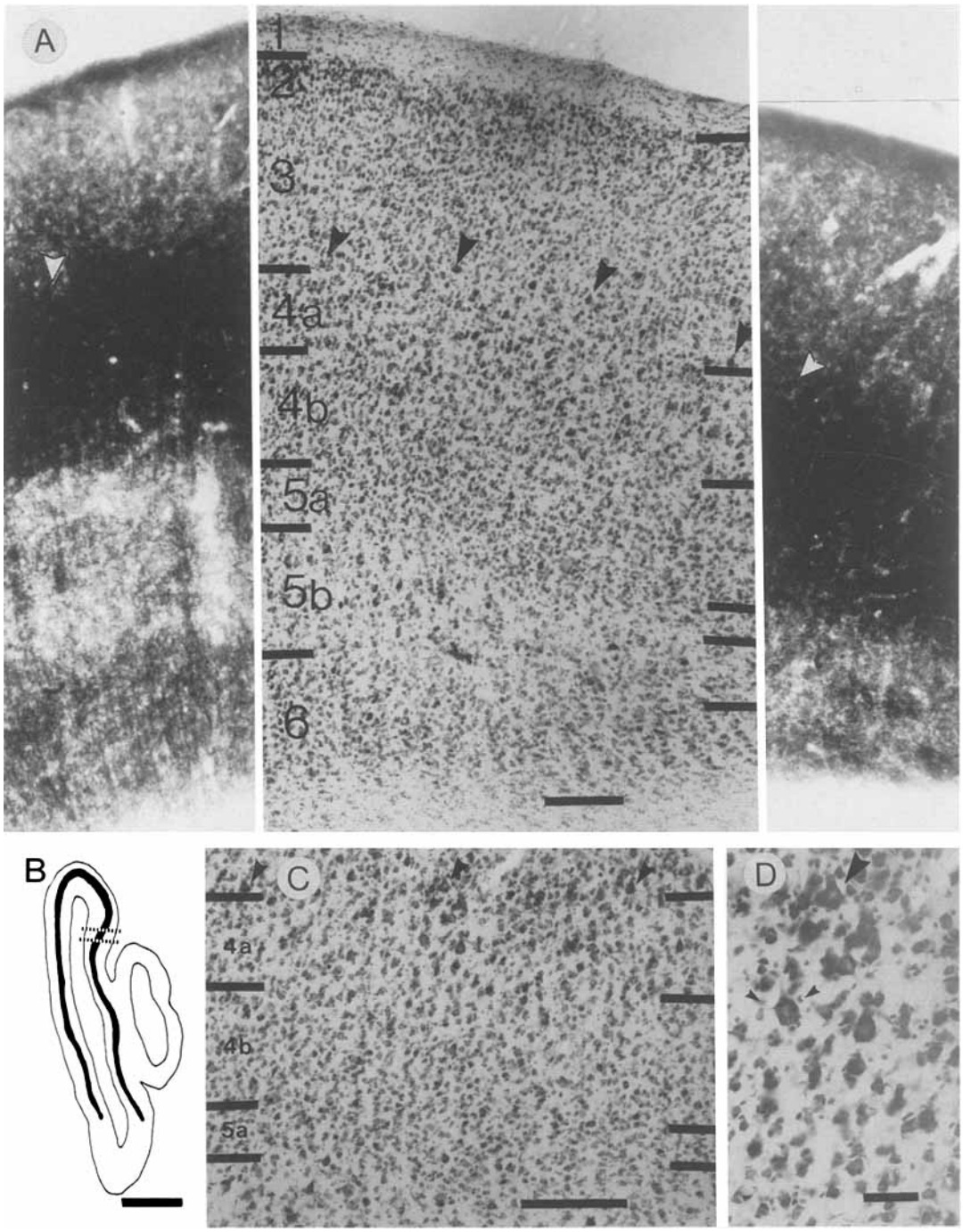

Fig. 3. Laminar pattern of cytochrome oxidase (CO) staining. The left and right panels of **A** show CO staining in coronal sections through areas 17 and 18, respectively. These photographs were matched to an adjacent section stained for Nissl substance with cresyl violet, in the middle panel. This section includes the 17/18 border, area 17 to the left, area 18 to the right. Arrowheads mark examples of large pyramidal cells at the layer 3/4 border, stained for Nissl or CO. Scale bar, 200 μm. A low power drawing of the CO stained section (A-P-2) photographed for A is shown in **B.** The 17/18 border is flanked by the dashed lines. Layer 4 is shown as a thick black line. Scale bar, 2 mm. A high power photomicrograph of layer 4 at the 17/18 border, area 17 to the left, area 18 to the right is shown in **C.** Arrowheads mark three examples of large pyramidal cells at the layer 3/4 border. Scale bar, 200 μm. The middle cell is shown at higher power in **D** (large arrowhead). Below this cell, in layer 4a, is a large cell, with dendrites (small arrowheads) radiating from the soma in the manner of a star-pyramid. Scale bar, 50 μm.

between layer 4a and layer 4b, determined cytoarchitectonically.

Figure 6D shows A laminae projections to area 18. In area 18, other studies have shown that Y axons in area 18 extend well into the lower part of layer 3 (Humphery et al., 1985a,b). We found that, as in area 17, geniculate terminals from the A layers were nearly completely confined to layers 4 and 6, and did not extend appreciably into layer 3 or layer

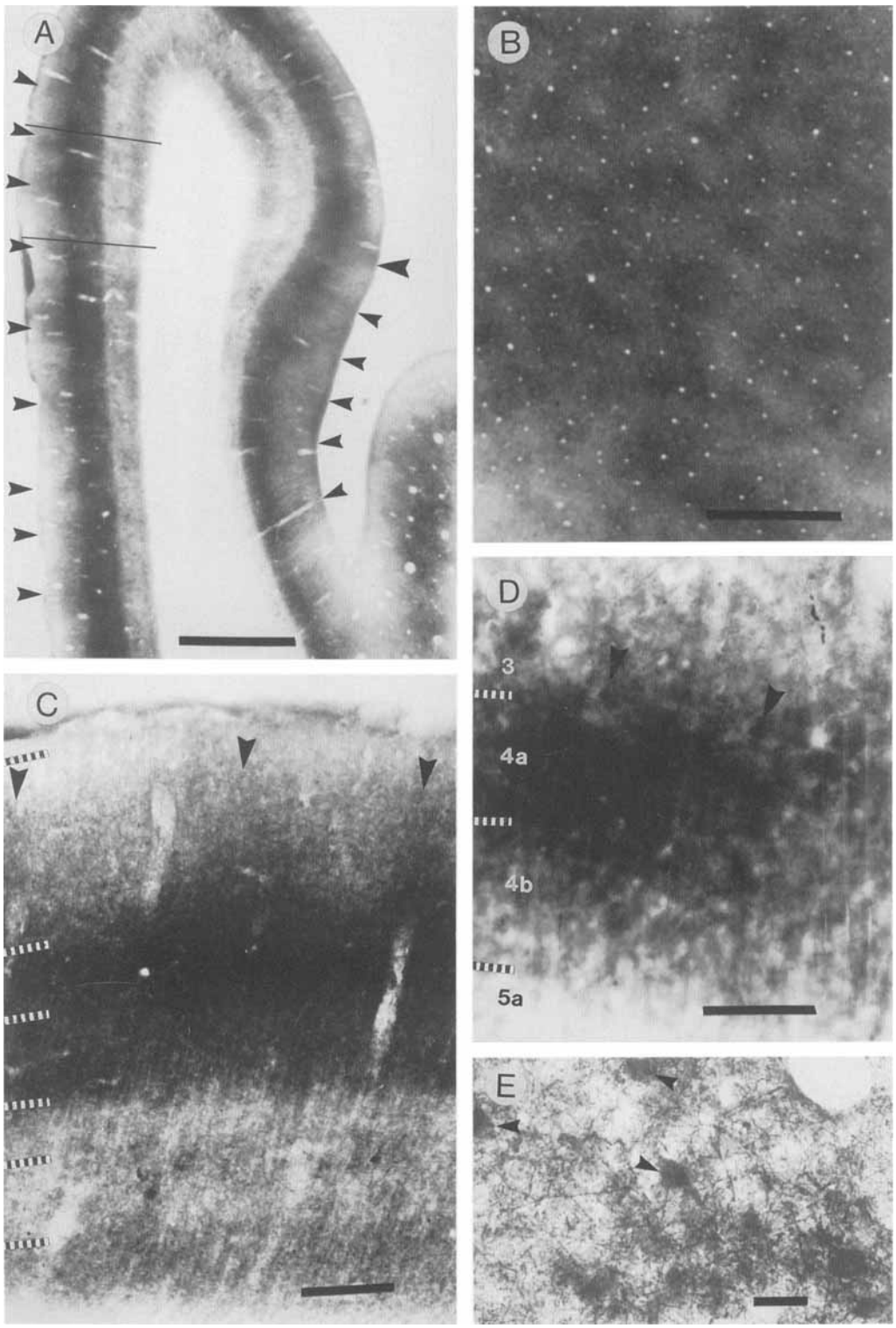

Fig. 4. CO blobs in coronal and tangential planes of section. **A:** A low magnification photograph of a CO stained section near-adjacent to the one shown in Figure 3B. The 17/18 border is marked by a large arrowhead. The small arrowheads mark examples of CO blobs, which appear as increases of labeling density in layers 3 and 4a, in both areas 17 and 18. The area between the solid black lines is shown enlarged in 4C. CO blobs are clearly visible in the tangential section through layer 4a of area 17 shown in **B.** Scale bars in A, B, 1 mm. **C:** Enlargement of the area between the solid black lines in A. Parts of three CO blobs are visible (arrowheads). Note that the blobs are visible in layer 4a as well as in layer 3. **D** shows a high power photomicrograph of layer 4. A CO blob is at the left, an interblob zone is at the right of this photo. Within the blob, layer 4a is more densely stained than layer 4b. In the inter blob, layer 4a is only slightly darker than layer 4b. The arrowheads mark two border pyramids staining for CO. Scale bar, 100 μm. The CO-stained border pyramids are seen more clearly in tangential sections through the layer 3/4 border (**E**). Truncated apical dendrites can be seen arising from some of these cells (arrowheads). Scale bar, 50 μm.

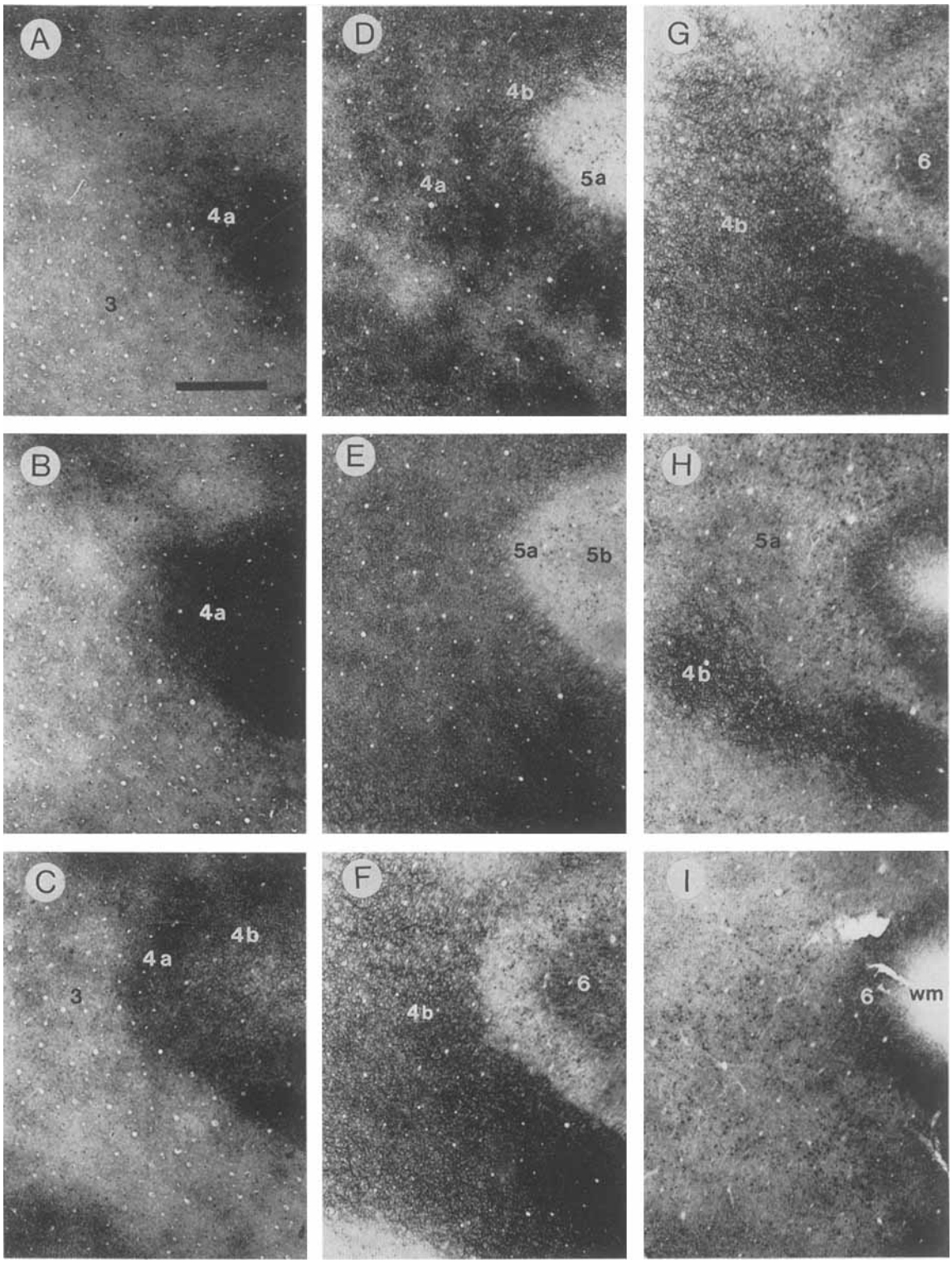

Fig. 5. A tangential series of 50 μm CO stained sections through area 17. Every other section, starting from the middle of layer 3 (A) and continuing to layer 6 (I) is shown. Cortical layers are numbered; "wm," white matter. Scale bar, 1 mm, and applies to **A–I.**

5a. Figure 6E shows a bright field photomicrograph of the layer 3/4 border in area 18, in a section counterstained for Nissl substance with neutral red. Three large border pyramids are shown, and it can be seen that these are above the zone of heavy geniculate terminations. Viewing the same field with more sensitive dark field optics, very sparse terminal labeling could be seen extending to a level just above the border pyramids, as was observed for A laminae

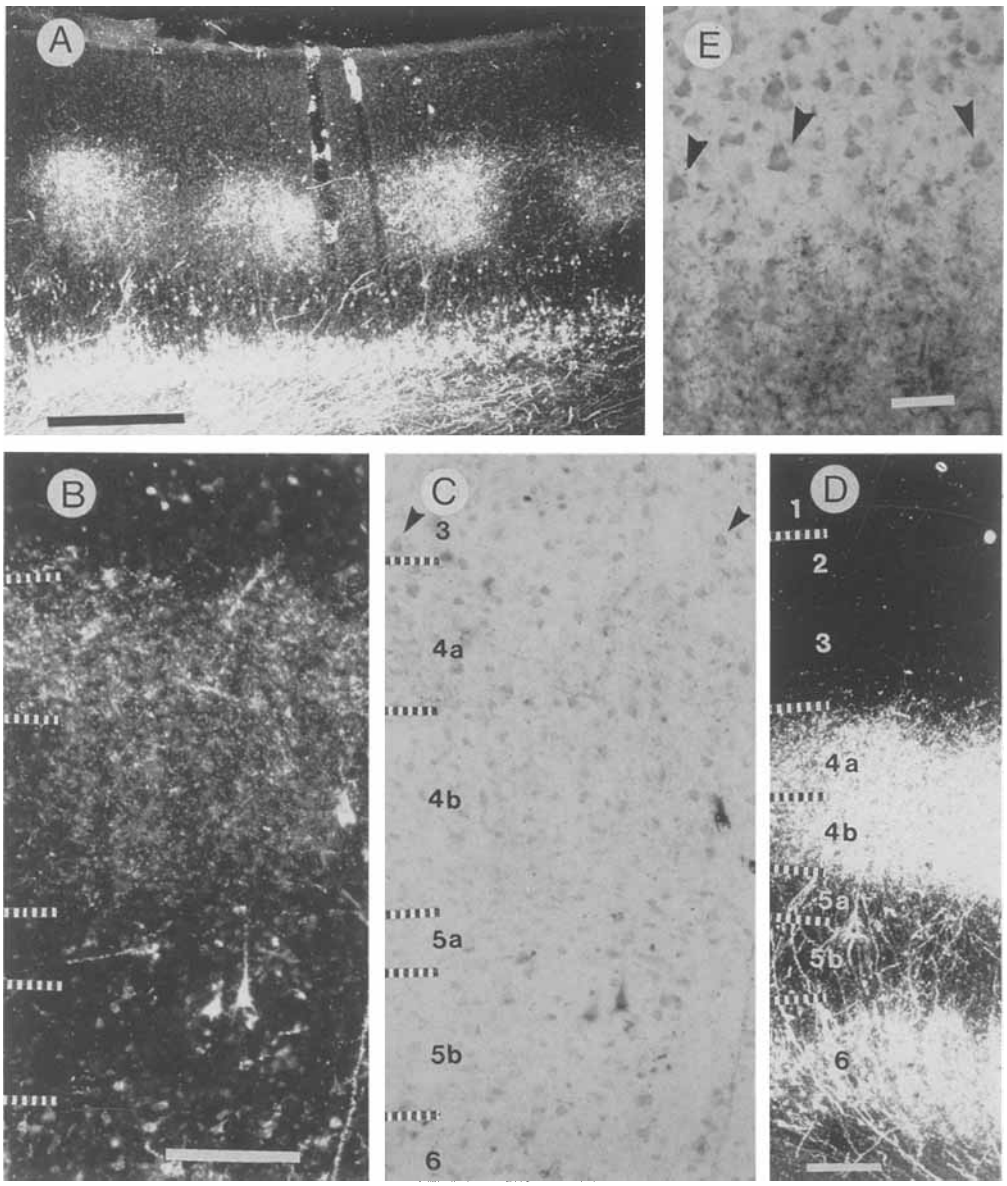

Fig. 6. Labeling from the A laminae in areas 17 and 18. **A:** A low magnification, darkfield photomicrograph of ipsilateral ocular dominance columns in area 17 resulting from WGA-HRP transport from lamina A1 of the LGN. Scale bar, 500 μm. **B:** A higher magnification darkfield photomicrograph of a single column of labeling. Note the difference in labeling density between the upper and lower parts of layer 4. Laminar boundaries are marked by dashed lines and laminae are numbered. Scale bar, 200 μm, and applies to both **B** and **C.** The same field of view is shown photographed in brightfield after counterstaining with neutral red in Figure 4C in order to show the neutral red counterstain. It can be seen that the change in density of labeled terminals between the upper and lower parts of layer 4 corresponds to the border between sublayers 4a and 4b. The arrowheads mark examples of border pyramids at the 3/4 boundary. **D:** A laminae labeling in darkfield illumination in area 18. Scale bar, 200 μm. **E:** A brightfield photomicrograph of the layer 3/4 border in area 18. The arrowheads mark 3 border pyramids counterstained with neutral red. Scale bar, 50 μm.

terminations in area 17. As was the case for the CO staining in area 18, the discrepancy between this study and previous ones probably involves differences in the assignment of the layer 3/4 border.

Labeling from the C laminae of the LGN in areas 17 and 18 had a different laminar pattern from labeling from the A laminae. Figure 7A shows a low power photomicrograph of labeling from the C laminae in area 17. Note that the labeling is patchy, with a spacing of 500–750 μm. As the labeling from the C laminae was always patchy, and the injections used were certainly large enough to include laminae C, C1, and C2, these patches were not likely due to projections to one set of ocular dominance columns as might be expected from injections into a single eye-specific layer. The C laminae are composed of a magnocellular layer C, which contains many Y-cells, and parvocellular layers C1 and C2 which contain mostly W-cells. The section shown in Figure 7A was taken from the A-P level corresponding to the transition between labeling arising from both divisions of the C laminae, as shown on the left, and labeling arising

from only the parvicellular divisions of the C laminae, as shown on the right. Note the two distinct patterns of labeling, that on the left including part of layer 4, and that on the right excluding layer 4. These two patterns of labeling are shown at higher magnification in Figure 7B,C. The patch of labeling on the left of Figure 7B has dense terminal labeling in layers 4a, 5a, and 1, and less dense labeling extending upwards several hundred microns from the top of layer 4 into the superficial layers. In the patch of labeling on the right in Figure 7B (arrowhead), the dense labeling in layer 4a is nearly absent, although labeling in 5a, 1, and the superficial layers is still present. The dashed line in Figure 7C indicates the subdivision of layer 4b, as described earlier, into a lower sublayer with smaller, more closely packed cells, and an upper division with slightly larger, less closely packed cells.

Figure 8A,C is a higher power photomicrograph of two further examples of patches of C laminae labeling in area 17. (Although most patches were labeled more densely than these, the less densely labeled patches were chosen for illustration as the lesser quantity of labeling did not obscure the Nissl staining. The more densely labeled patches had the same laminar distribution.) When compared to the matching Nissl stain shown in brightfield, it can be seen that the patches span the border of layers 3 and 4, with the labeling in upper layer 4 being more dense than the labeling in layer 3. Although the labeling in layer 4 was mostly confined to layer 4a, there was occasionally some faint labeling in layer 4b; note, however, that this labeling is restricted to the upper part of layer 4b, and does not extend into the lower zone of small cells in this layer. The extent of labeling in layer 3 varied from section to section, but in some cases extended to near the top of layer 3. A narrow band of labeling in layer 5a was also present, and this was patchy as well, although not always as clearly, with the layer 5a patches in register with those in layer 3/4. As well as the patchy labeling in other layers, there is a thin, continuous band of labeling confined to the top half of layer 1, and continuous, mostly retrograde, labeling in layer 6.

The photomicrographs in Figure 9 were taken from sections at the anterior-most extent of the cortical labeling, and thus at the most negative visual field elevation labeled in the cortex. Figure 9A,B,D shows patches of labeling in darkfield. Figure 9C is a bright field micrograph of the same field of view shown in Figure 9B. Figure 9E,F are higher magnification micrographs, in darkfield and brightfield, respectively, of the patch of labeling on the right side of Figure 9D. In all cases, although labeling in layers 3, 5a, and 1 is present, labeling in 4a is absent, or very sparse. Because this pattern was found at the lowest iso-elevation representation labeled, it suggests that the labeling originated from the bottom of the C laminae, where the lowest iso-elevation representations were injected. Thus, the small W cells of layers C1 and C2 appeared to project to patches in layer 3, while the large Y cells in the top part of the C-layers projected to patches in layer 4a precisely in register with the projection to layer 3.

As in area 17, patches of terminals spanning layers 3 and 4 were also present in area 18 following C-laminae injections (Fig. 10A,B). However, in area 18 the dense labeling in layer 4 extended throughout the entire depth of the layer and was not confined to layer 4a (Fig. 10C). Moreover, while the terminal patches in layer 3 were as pronounced as those in area 17, the labeling in layer 4 tended to be less patchy than in area 17. When patches of increased labeling density were present in layer 4, however, they were always in register with patches in layer 3. The labeling in layer 5a in area 18 was also patchy, as in area 17, even when the labeling in the intervening layer 4 was nearly continuous, and these patches were also always in register with the patches in layer 3 (Fig. 10B).

In some sections, labeling from both the A laminae and the C laminae was present in the same visual field representations. The differences in laminar distribution of the projections of these two divisions of the LGN made it possible to examine the relationship of patches of C laminae labeling to the ocular dominance columns shown by A laminae injection. Similar to Figure 7, Figure 11A shows a transition in labeling pattern, this time from laminae A1 labeling (on the left of the micrograph) to C-laminae labeling (on the right). In the center of the figure, both labeled ocular dominance columns from lamina A1 (black arrowheads) and the C-laminae patches (white arrowheads) are present. The C-laminae patches are found over both contralateral and ipsilateral ocular dominance columns, and at least one C-laminae patch straddles the border of an ocular dominance column. Another example of concurrent lamina A1 and C-laminae labeling is shown in Figure 11B. In this example, one patch of C-laminae labeling (white arrowhead) is centered over a labeled ocular dominance column (black arrowhead), and another patch of C-laminae labeling is centered over an unlabeled column.

Tangential organization of geniculocortical projections

The relationship between the patches of geniculate labeling from the C laminae and the CO blobs was examined in sections cut tangential to the cortical surface. Figures 12, 13, and 14 show labeling from the C layers of the LGN in tangential sections. In each case, sections reacted for HRP to visualize thalamic afferents were aligned with sections reacted for CO to visualize the blobs, using the pattern of radially penetrating blood vessels. Figure 12A shows an example of labeling from the C layers of the LGN in layer 3 of area 17. The labeling is arranged in patches with a center-to-center spacing of slightly less than 1 mm. Often, the patches align to form rows, with bridges of labeling connecting patches in a row. A similar pattern of patches, or blobs, with connecting bridges is seen in the section stained for CO in Figure 12B. The positions of patches of C-laminae labeling and CO blobs were found, most often, to correspond. Some examples of correspondence between patches of labeling and CO blobs in Figure 12 are numbered. Except for the top right part of Figure 12B, where the plane of section passes out of layer 4 into layer 5, there is good correspondence between the patches of anterograde labeling and the CO blobs.

Figure 13 shows, from a different experiment, another example of the relationship between labeling from the C layers of the LGN and CO blobs in area 17. In this case, the sections shown are not from layer 3, but from layer 4a. Note that the patches of anterograde labeling are more dense and have a slightly larger diameter than those in layer 3, but that they have a similar spacing. (The greater density of labeling in layer 4a versus layer 3 was also noted in the coronal sections.) Likewise, the CO blobs in layer 4a are more robust than, but have a similar spacing to, those than in layer 3. As in layer 3, there is good correspondence between the patches of anterograde labeling and the CO blobs in layer 4.

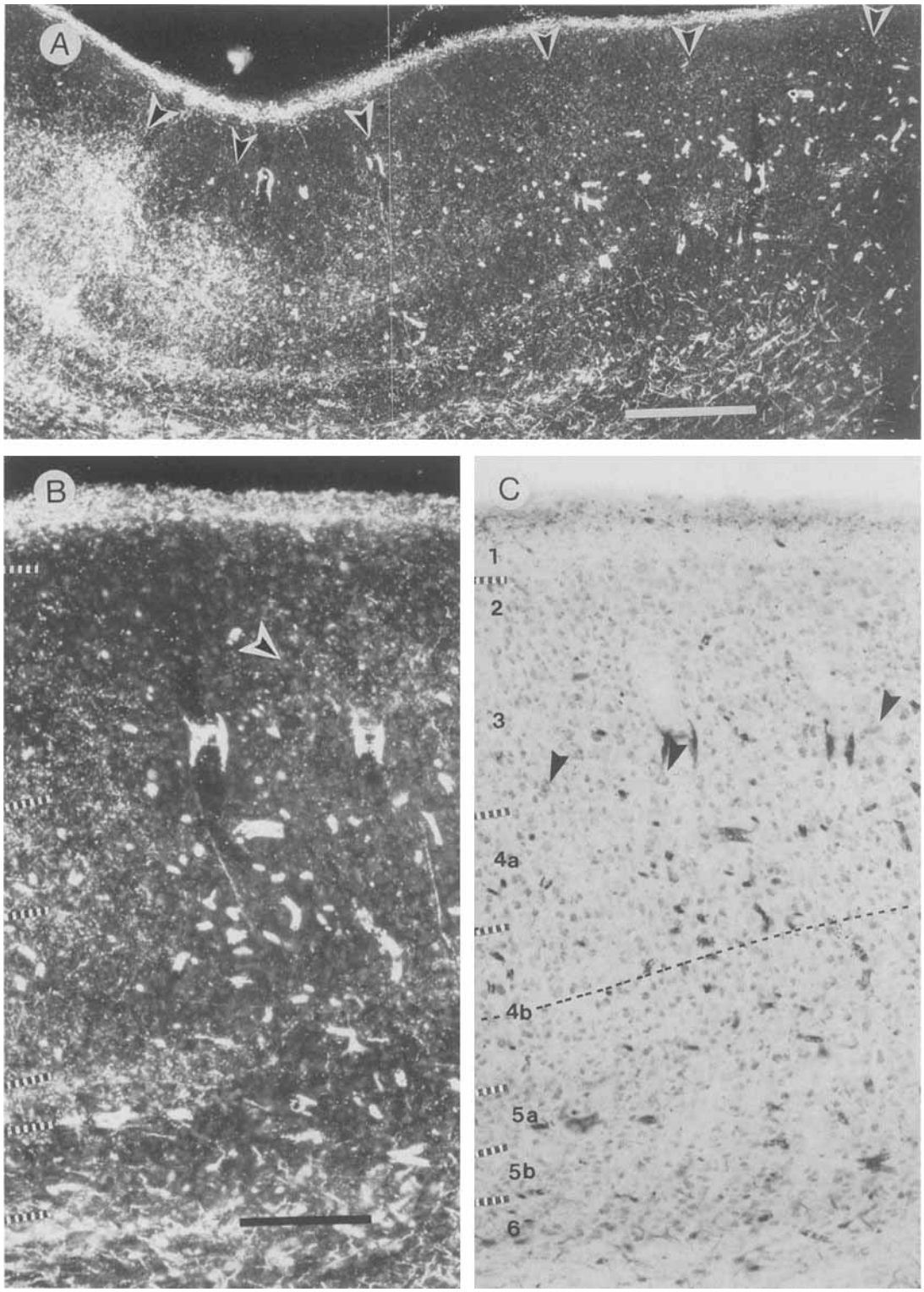

Fig. 7. Labeling from the C laminae in area 17. **A:** A low magnification darkfield photomicrograph of C laminae labeling in area 17. Arrowheads show individual patches of labeling. This figure shows the transition between two distinct patterns of labeling, that on the left including part of layer 4, and arising from both divisions of the C laminae, and that on the right excluding layer 4, and arising from only the parvicellular divisions of the C laminae. Scale bar, 500 μm. **B, C:** At higher magnification, another example of the transition to parvicellular C-laminae labeling. B: A darkfield photomicrograph of anterograde labeling. C: The same field of view photographed in brightfield to show the cytoarchitecture. The patch of labeling on the left in B has dense terminal labeling in layers 4a, 5a, and 1, and less dense labeling extending upwards several hundred microns from the top of layer 4 into the superficial layers. In the patch of labeling on the right, the dense labeling in layer 4a is nearly completely absent, although labeling in 5a, 1, and the superficial layers is still present. In C, arrowheads mark examples of border pyramids. The dashed line indicates a subdivision of layer 4b into a lower sublayer with smaller, more closely packed cells, and an upper division with slightly larger, less closely packed cells. Scale bar, 200 μm and applies to B and C.

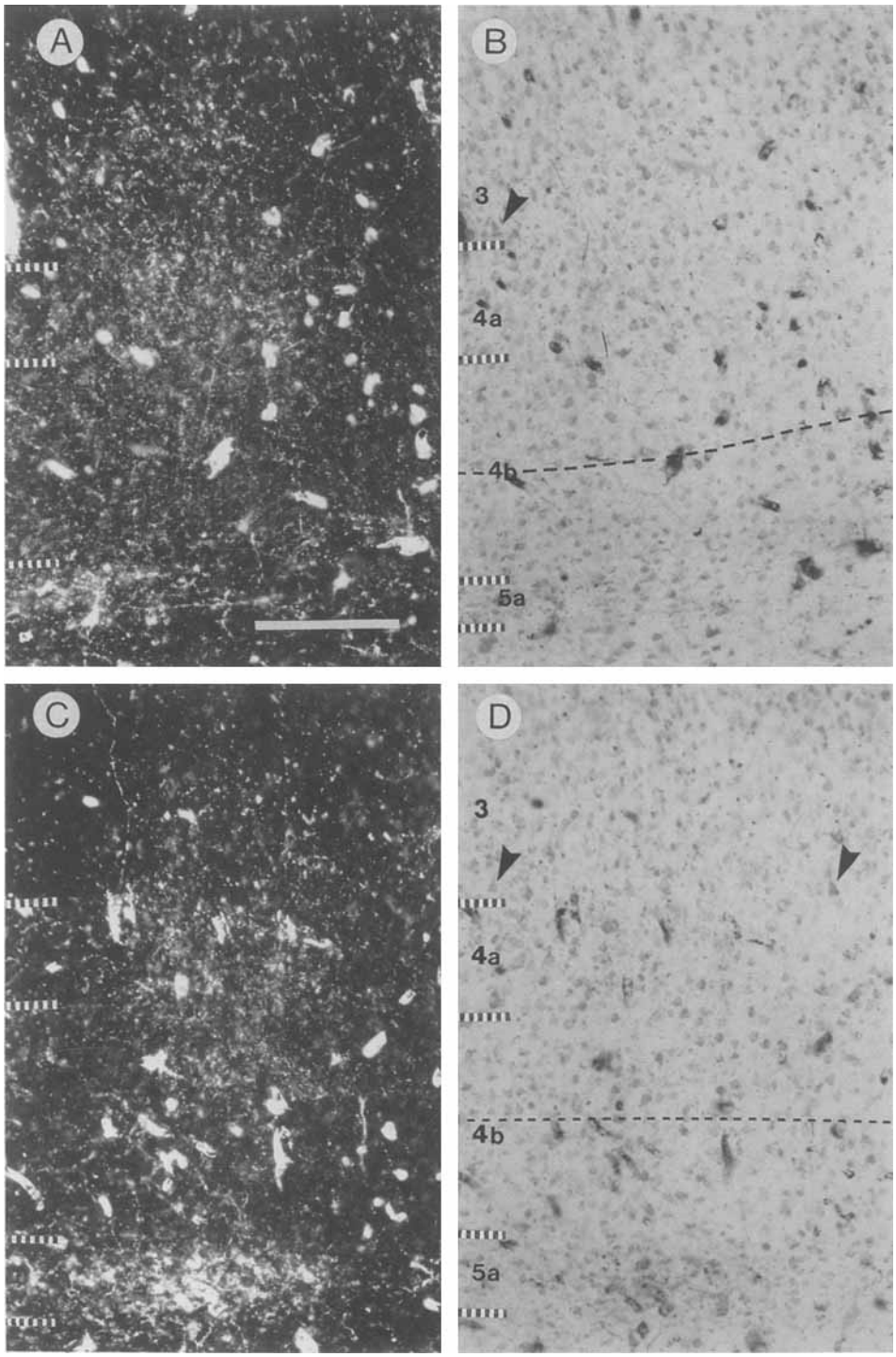

Fig. 8. Two more examples, at higher magnification, of patches of C-laminae labeling in area 17. **A, C:** Darkfield photomicrographs of anterograde labeling. **B, D:** Matching brightfield micrographs. Arrowheads mark examples of border pyramids. The dashed line indicates the subdivision of layer 4b into lower and upper sublayers. Labeling is denser in layer 4a than in the superficial layers. There is also some faint labeling in layer 4b, but note that this is restricted to the upper part of layer 4b, and does not extend into the lower, smaller celled part of the layer. Scale bar, 200 μm and applies to A–C.

Figure 14 shows that the relationship between patches of labeling from the C layers of the LGN and CO blobs is also present in area 18. The section in 12A is from layer 3, and the section in 12B grazes the layer 3/4 border. In area 18, the spacing of both the patches of anterograde labeling and the CO blobs was slightly larger than in area 17. The patches of anterograde labeling, and especially the CO blobs, were not as well defined as those in area 17. However,

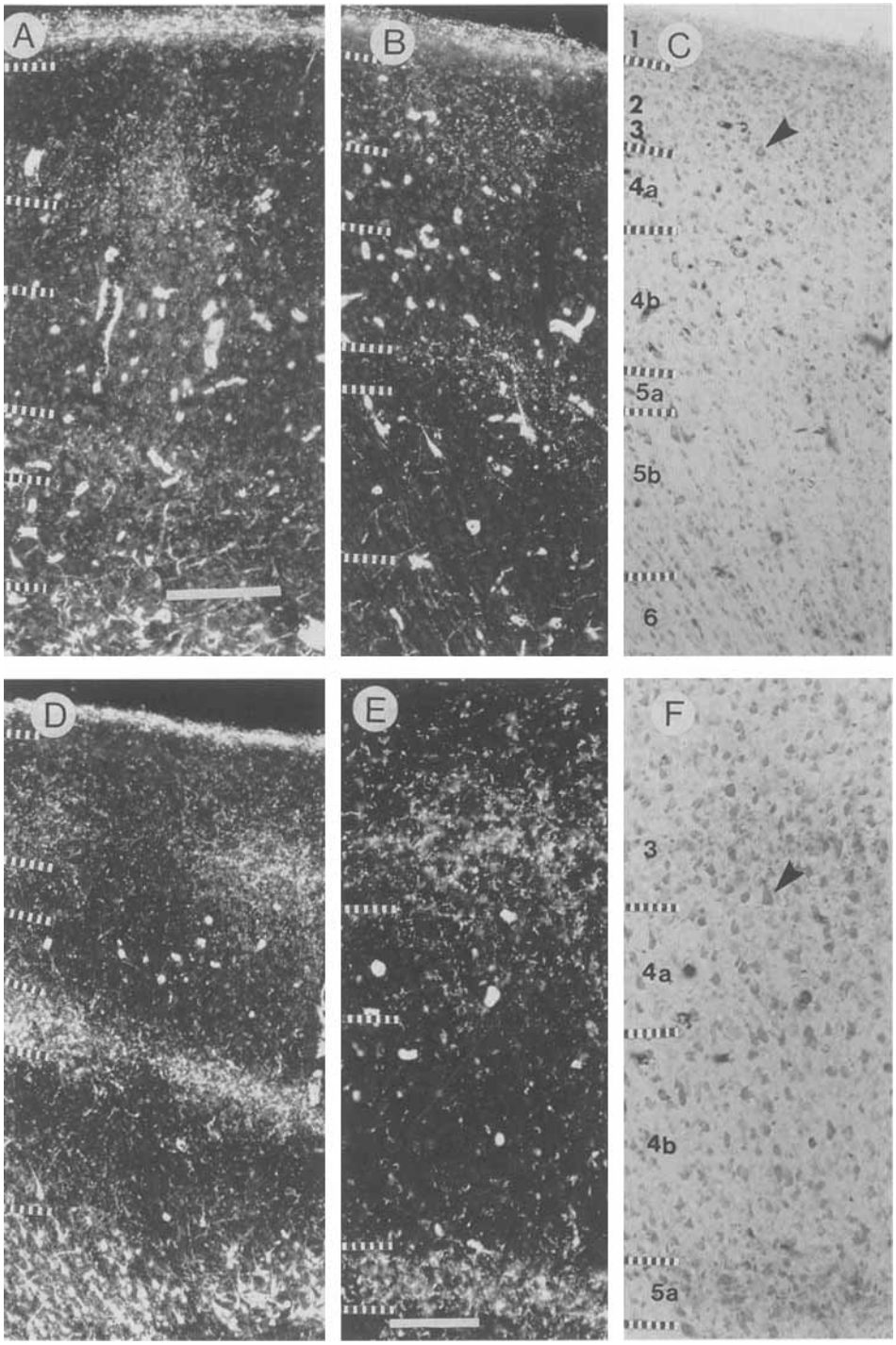

Fig. 9. More examples of parvicellular C-laminae labeling in area 17. **A, B, D**: Patches of labeling in darkfield. Scale bar in A, 200 μm and applies to A–D. **C:** A brightfield micrograph of the same field of view shown in B. The arrowhead marks a border pyramid. Note that labeling in 4a is absent, or very sparse. **E, F:** Higher magnification micrographs, in darkfield and brightfield, respectively, of the patch of labeling on the right side of D. The arrowhead indicates a border pyramid. Again, note the patch of labeling in layer 3, and the lack of labeling in layer 4a. Scale bar, 100 μm and applies to E–F.

the correspondence between the anterograde labeling and the CO staining was still reasonably good.

In order to quantify the correspondence between C-laminae labeling and CO staining, digitized computer images of the labeling patterns shown in Figures 12 to 14 were made. As described in the "Materials and Methods" section, linear regression was used to measure the strength of the correlation between pixel brightness values in corresponding locations of each pair of images. For each of the three pairs of images, there was a significant negative

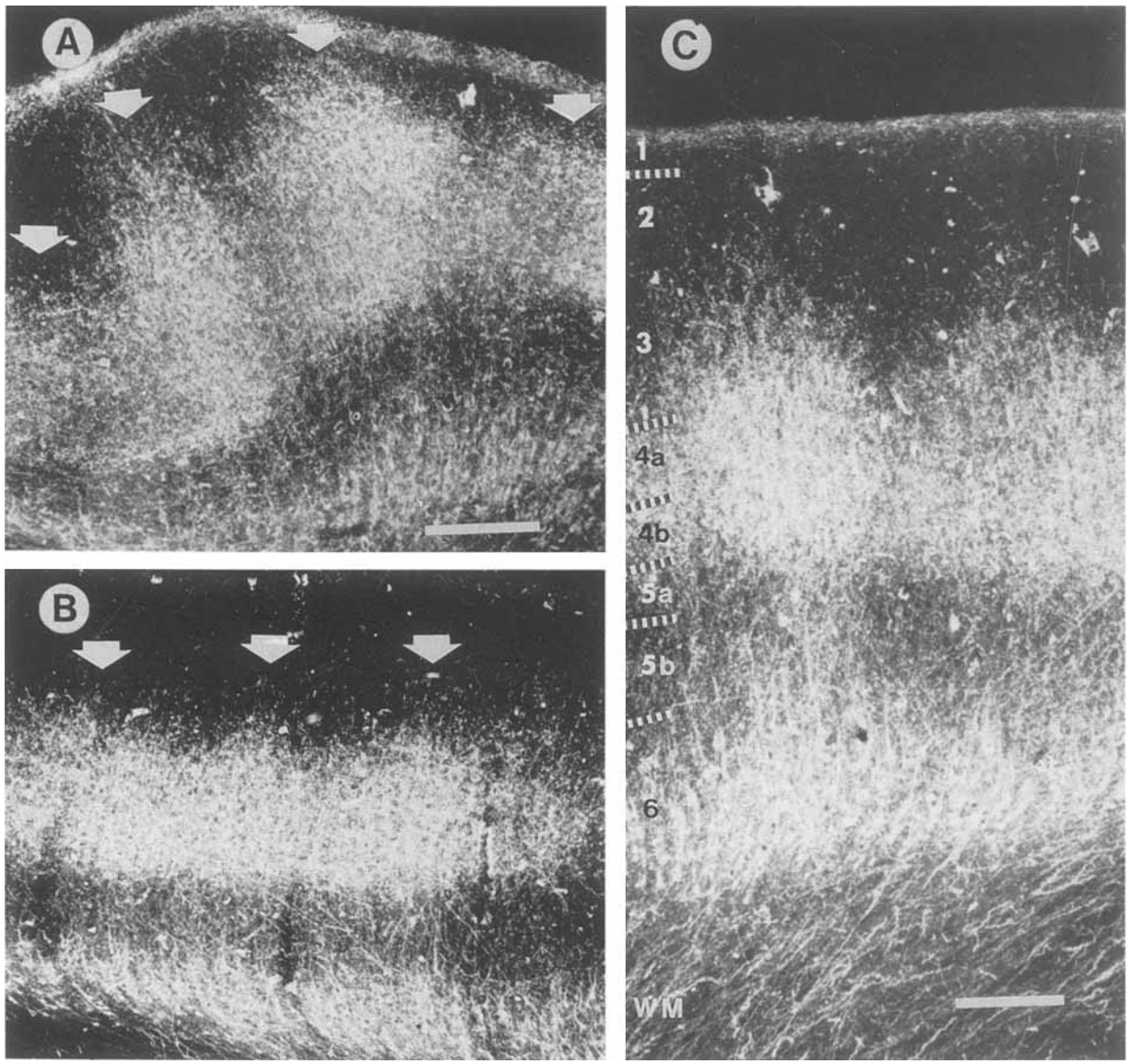

Fig. 10. Labeling from layer C in area 18. A, B: Low magnification darkfield photomicrographs of C laminae labeling in area 18. The arrows mark patches of labeling in layer 3. In A there are dense patches of labeling in layers 4a and 4b aligned with those in layer 3; in B, layer 4 is nearly continuously labeled. Scale bar, 500 μm, and applies to both A and B. C shows the labeling pattern at higher magnification. Laminar boundaries are marked by dashed lines. Scale bar, 200 μm.

correlation between pixel brightness values in the CO- and HRP-stained sections, with $P < 0.001$.

DISCUSSION

We examined the pattern of geniculocortical terminations in the cat's visual cortex. It was desirable for this study to examine geniculocortical projections arising from particular classes of geniculate cells, in isolation from labeling of other cell classes. In the cat LGN, X, Y, and W cells are only partially segregated into different lamina. The two largest geniculate layers, layers A and A1, contain a mixture of X and Y cells. The C layers, ventral to the A layers, can be subdivided into an upper, magnocellular division (layer C) containing both Y and W cells, and a lower, parvicellular division (layers C1 and C2) containing mostly W cells. Knowing the laminar distribution within the LGN of the various cell types, it is possible to analyze our results from bulk injections of tracers into particular lamina in terms of X, Y, and W projections (Fig. 15).

Laminar pattern of geniculocortical terminations

The input from the A laminae, containing X and Y cells, was confined to layers 4 and 6 in areas 17 and 18. Other studies have suggested that Y cell projections might extend several hundred microns into layer 3, especially in area 18 (Humphery et al., 1985b). These discrepancies are probably due to the use of different laminar schemes and to the

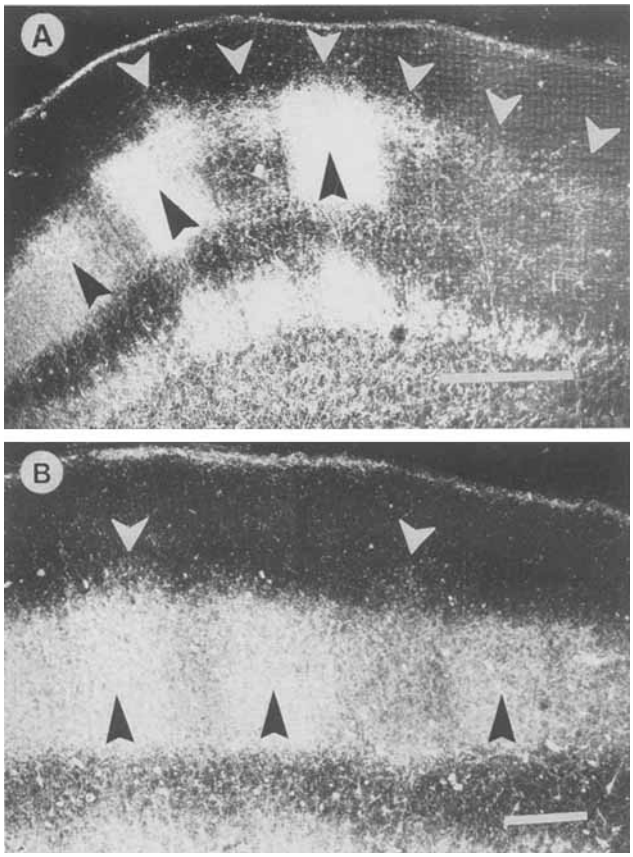

Fig. 11. Comparison of C-laminae labeling and A-laminae labeling in the same sections. **A:** The transition from patches extending throughout layer 4, characteristic of lamina A1 labeling (on the left of the micrograph) labeling from the C-laminae (on the right). In the center of the figure, both labeled ocular dominance columns from lamina A1 (black arrowheads) and the C-laminae patches (white arrowheads) are present. The C-laminae patches are associated with columns labeled from lamina A1, as well as with columns not labeled from A1; at least one C-laminae patch straddles the border of a column labeled from A1. Scale bar, 500 μm. Another example of lamina A1 and C laminae labeling in the same section is shown in **B.** As in A, black arrowheads mark ipsilateral ocular dominance columns labeled from layer A1 and white arrowheads mark patches of labeling from the C laminae. In this example, the leftmost patch of C-laminae labeling is centered over a labeled ocular dominance column, while the rightmost patch of C-laminae labeling is centered over an unlabeled column. Scale bar, 200 μm.

inconsistent usage of the same scheme between different studies. For instance, the small pyramidal cells of O'Leary's (1941) layer 5a have been considered both equivalent to (Garey, 1971), and excluded from (LeVay and Gilbert, 1976), layer 4c of Otsuka and Hassler's (1962) lamination scheme, according to different authors.

Regarding the Y cell projections in layer 3 of area 18 reported by Humphery et al. (1985), their layer 3/4 border appears to correspond to O'Leary's 4a/4b border, as the cells marked "border pyramids" in their Figure 7 are smaller than some pyramidal cells in the figure that are several hundred microns more superficial in the cortex. This scheme of area 18 lamination appears to be related to the fact that the cells in layer 4a of area 18 are larger than their counterparts in area 17 and were thus considered a sublayer of layer 3 (layer 3b) by Otsuka and Hassler (Otsuka and Hassler, 1962). Size aside, however, the cell types of this layer, including the star pyramids, are similar in areas 17 and 18, as noted in Golgi studies by Lorente de Nó (Lorente de Nó, 1943). As previously mentioned, use of this scheme also appears to account for the claim that the band of dense CO staining spans the layer 3/4 border in area 18 (Price, 1984). Regardless of whether it should be termed layer 4a or layer 3b in area 18, this sublayer is marked by similar cytology, geniculate A laminae inputs, and dense CO staining in both area 17 and area 18.

The input from the C layers was segregated into an upper and a lower tier in the visual cortex, straddling the A lamina input in layer 4. Our findings concerning the lower tier of labeling contrast slightly with those of LeVay and Gilbert (1976), who concluded that these projections straddle the layer 4/5 border. This may have been due, in part, to the scheme of cortical lamination used (see above). Also, it can be difficult to determine this border in Nissl stained sections, although it was very clearly marked in the alternate sections stained for CO in this study. This lower tier of C laminae labeling appears to specifically target the small pyramidal cells of layer 5a. It would be interesting to examine closely the response properties of cells in layer 5a for physiological evidence of this W-cell projection.

We were also able to show that the upper tier of labeling, straddling the layer 3/4 border, is actually composed of two components, since labeling from the parvicellular C layers projected to layer 3 (and also layers 5a and 1), but not to layer 4. Therefore, the labeling in layer 4 appears to arise from the Y-cells in layer C, and the labeling in layer 3 from the W-cells in layers C1 and C2. The projection of the parvicellular C laminae (C1 and C2) to layers 3 and 5, but not layer 4, of area 17 was also suggested by small injections of tracers restricted to individual cortical layers (Leventhal, 1979). Thus, W-cell appears to be completely segregated from cortical cell layers receiving X- and Y-cell input (Fig. 15).

Geniculate inputs and cytochrome oxidase staining

The relationship of geniculate inputs to CO staining was also examined. It has been suggested that levels of CO staining in different cortical layers are related to the levels of activity of the particular geniculate inputs that they received. The close correspondences between the dense band of CO staining in layer 4 and the terminations of the more active X- and Y-cells from the LGN and between the lesser CO staining in layers 3 and 5a and the terminations of the less active W-cells are consistent with this. Our data appear to extend this relationship between CO staining and geniculate inputs to comparisons of different cortical columns, as well as layers. In particular, the CO blobs were shown to be specifically targeted by the projections from the C layers of the LGN. The differences in CO staining between blobs and interblobs could be seen in layer 3, where W-cell terminations are made, and also in layer 4a, where the Y-cells from magnocellular layer C terminated.

It is suggested that, in each layer, the difference in CO staining between blob and inter-blob is due to the presence of a geniculate input in the blobs that is not present in the interblobs. In layer 3, this is readily apparent, as there is no geniculate input to layer 3 in the interblobs. In layer 5a, there is a patchy geniculate input aligned with the blobs in the supragranular layers, but no CO staining. It is possible that the W-cell input to layer 5a arises from a different class of W-cells in the C layers, which have lower levels of activity

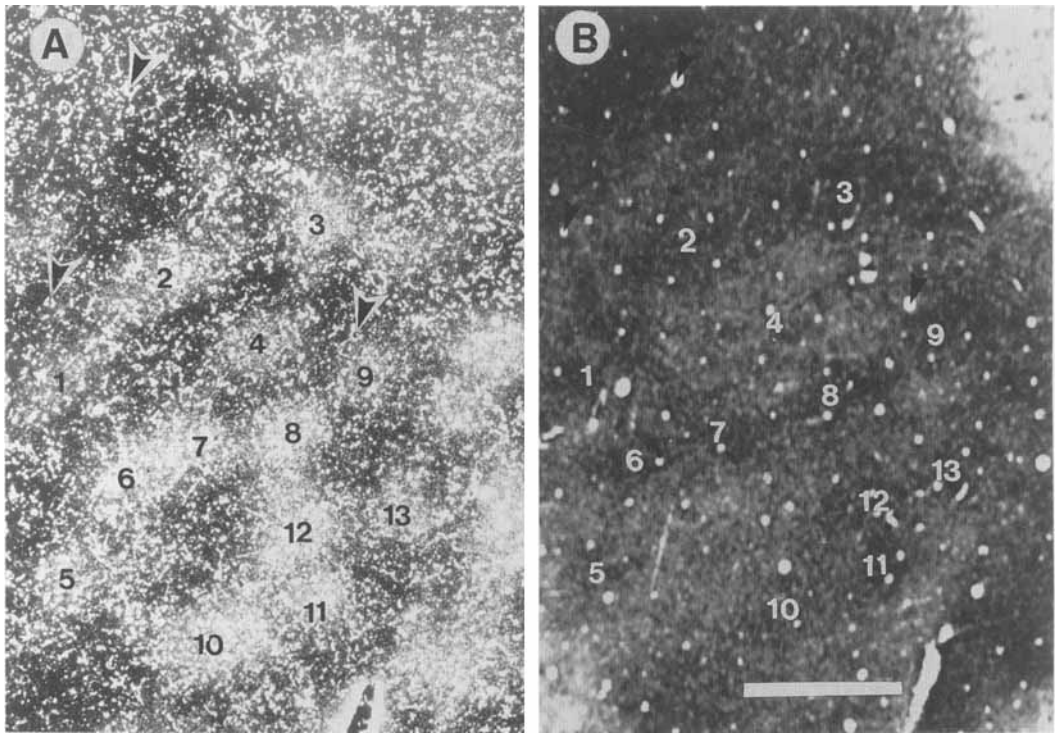

Fig. 12. Comparison of cytochrome oxidase blobs and C-laminae labeling in layer 3 of area 17. **A:** A darkfield photomicrograph of a tangential section through the lower part of layer 3 in area 17 containing peroxidase labeling arising from the lateral geniculate C laminae. **B:** A section from deeper in the cortex reacted for cytochrome oxidase. When patches of labeled terminals are compared to CO blobs, the two are most often found to align. Some examples of correspondence between the two patterns are numbered. Arrowheads show matching blood vessels used for alignment between the two sections. Scale bar, 1 mm, and applies to both A and B.

than those that project to the blobs in layer 3. It is known that W-cells in the parvicellular C laminae are physiologically heterogeneous and that several morphologically identified subclasses (gamma, epsilon, g1, and g2) of retinal "W-cells" project there (Leventhal, 1982).

In layer 4, although there is obviously geniculate input to and dense CO staining in both blobs and interblobs, this study showed that the Y-cells from the C layers terminate only in the blobs. As Y-cells in the LGN have moderately high spontaneous and evoked activity (Wilson et al., 1976; Bullier and Norton, 1979), and also stain more darkly for CO than X-cells (Kageyama and Wong-Riley, 1985), it is suggested that Y-cell input is responsible for the more dense CO staining in layer 4a blobs vs. interblobs. The less dense CO staining in the remainder of layer 4 would then be due to X-cell terminations. At present, it is not known if Y-cells in the A layers of the LGN also selectively target the CO blobs, as is the case for those from the C layers. This question was not possible to address with the bulk injections used in this study, as the A layers contain a mixed population of X-cells and Y-cells so it was not possible to selectively label either population alone. Experiments combining intracellular staining of identified Y-cells from the A laminae with CO histochemistry are needed to answer this question.

Although there is currently no data on the relationship of Y-cell projections from the geniculate A layers to the CO blobs, it is interesting to note that in many other respects A-layer projections show few differences from the Y-cells in the C layers of the LGN. Since single retinal Y-cell axons often send collaterals to lamina A, lamina C, and the MIN (Bowling and Michael, 1980; Sur et al., 1987), it is not surprising that Y-cells in all of these regions have similar physiological response properties (Dreher and Sefton, 1979). Also, the morphology of the geniculocortical arborizations of Y-cells from the various parts of the LGN appears similar (Humphery et al., 1985a,b). Intracellular injection of HRP has shown that geniculocortical arbors of Y-cells from the A layers, layer C, and the MIN (but not X-cells) possess a patchy distribution of terminals (Humphery et al., 1985a,b). While thought to be due exclusively to the spacing of ocular dominance columns, this patchiness might also be due to the spacing between CO blobs. One difference in connectivity of A and C layer Y-cells is that a small percentage of presumed Y-cells (based on soma size) in layer C and the MIN project to extrastriate visual areas whereas essentially no cells in the A layers do (Tong et al., 1982). [Some A layer cells do project to extrastriate areas in the kitten, but these appear to be lost during development (Bruce and Stein, 1988; Tong, 1991)]. Thus, there is little reason to suspect that Y-cells in layers A and C should have different projection patterns in visual cortex. Concentration of Y-cell input in the blobs is also suggested by our recent results showing that clusters of cells projecting from area 17 to the posterior medial lateral suprasylvian area (Shipp and Grant, 1991) are concentrated in the CO blobs (Boyd and Matsubara, 1992); this area is thought to be dominated by Y-cell input (Berson, 1985; Rauschecker et al., 1987).

Because there is no segregated population of X-cells in the LGN, we were not able to examine X-cell terminations in isolation in this study. However, comparing the results of

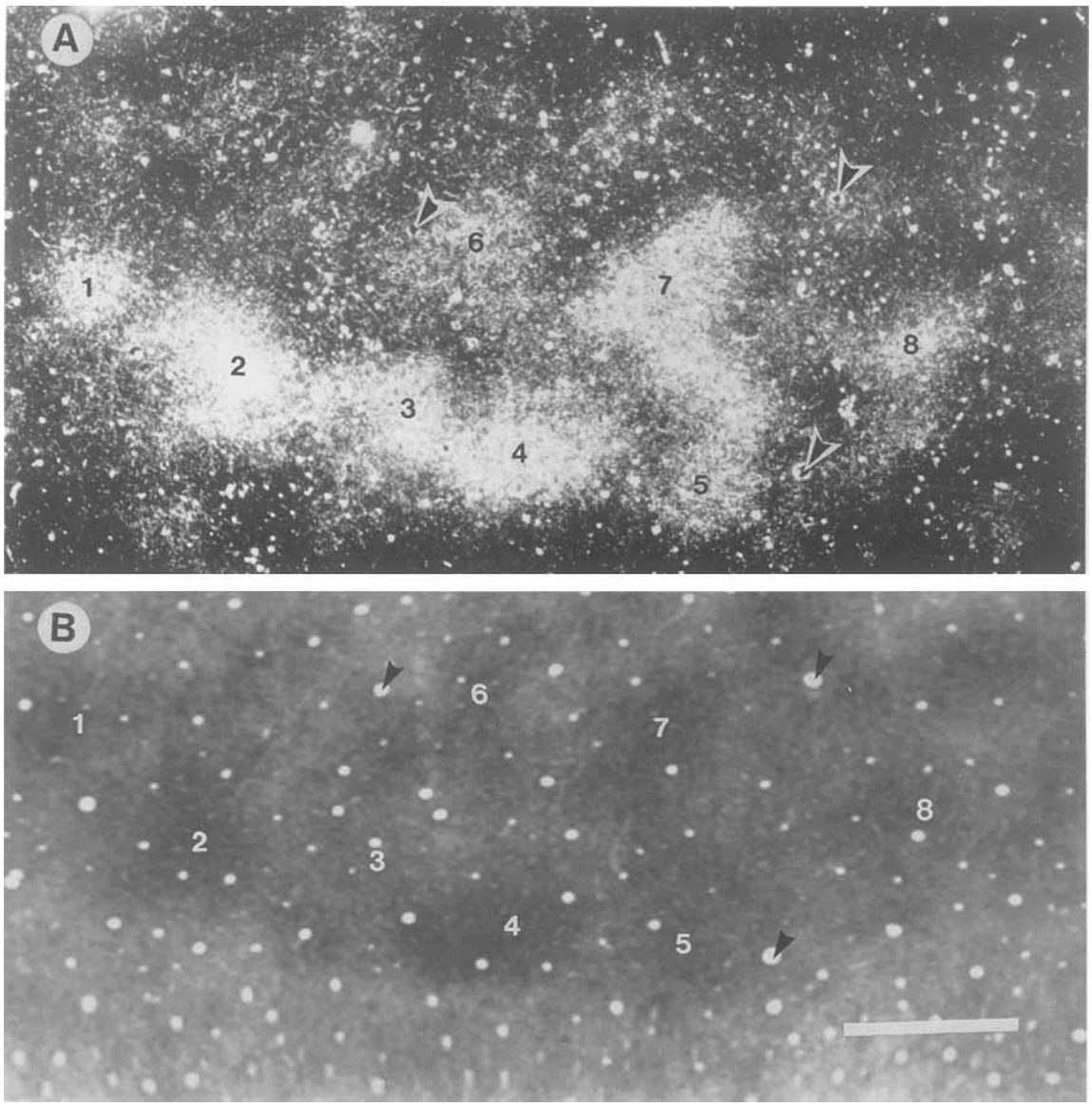

Fig. 13. Comparison of cytochrome oxidase blobs and C-laminae labeling in layer 4a of area 17. **A:** A tangential section through the layer 4a in area 17 reacted for peroxidase. **B:** An adjacent section reacted for cytochrome oxidase. As in Figure 12, examples of correspondence between the patches of anterograde labeling and the CO pattern are numbered. Arrowheads mark common blood vessels used for alignment. Scale bar, 1 mm, and applies to both A and B.

the C-laminae and A-laminae labeling (and assuming that the Y-cell terminations from layer C are representative of all geniculate Y-cell terminations), it appears that X-cell terminations must include both 4a and 4b in the interblobs and at least 4b underneath the blobs. It is not possible to tell, from the results of this study, whether intermingling of X-cell terminals and Y-cell terminations occurs in the layer 4a blobs, or whether X-cell terminations avoid the blobs altogether. A marker for X-cell terminals has recently been tentatively proposed, however (Dyck and Cynader, 1993a). Receptor autoradiography has shown that mesulergine (a selective ligand for the serotonin 1c receptor) binding in the visual cortex disappears after lesions of the LGN. This suggests that these receptors, like nicotinic acetylcholine receptors (Prusky et al., 1987), are located on LGN terminals. Unlike the nicotine receptors, which were present throughout the thickness of layer 4 in both areas 17 and 18, the serotonin 1c receptors were restricted to area 17, mirroring the distribution of X-cell terminations. Moreover, binding was different in the two sublayers of layer 4, forming a continuous band in layer 4b, with evenly spaced columns extending into layer 4a. Comparison with CO staining showed that these columns precisely interdigitated with the CO blobs (Dyck and Cynader, 1993b). If serotonin 1c receptors truly mark X-cell terminals, it would suggest that X-, Y-, and W-cell terminations are largely segregated within the cat's visual cortex. A schematic diagram illustrating the laminar and columnar terminations of LGN X, Y, and W-cells demonstrated in this study is shown in Figure 15.

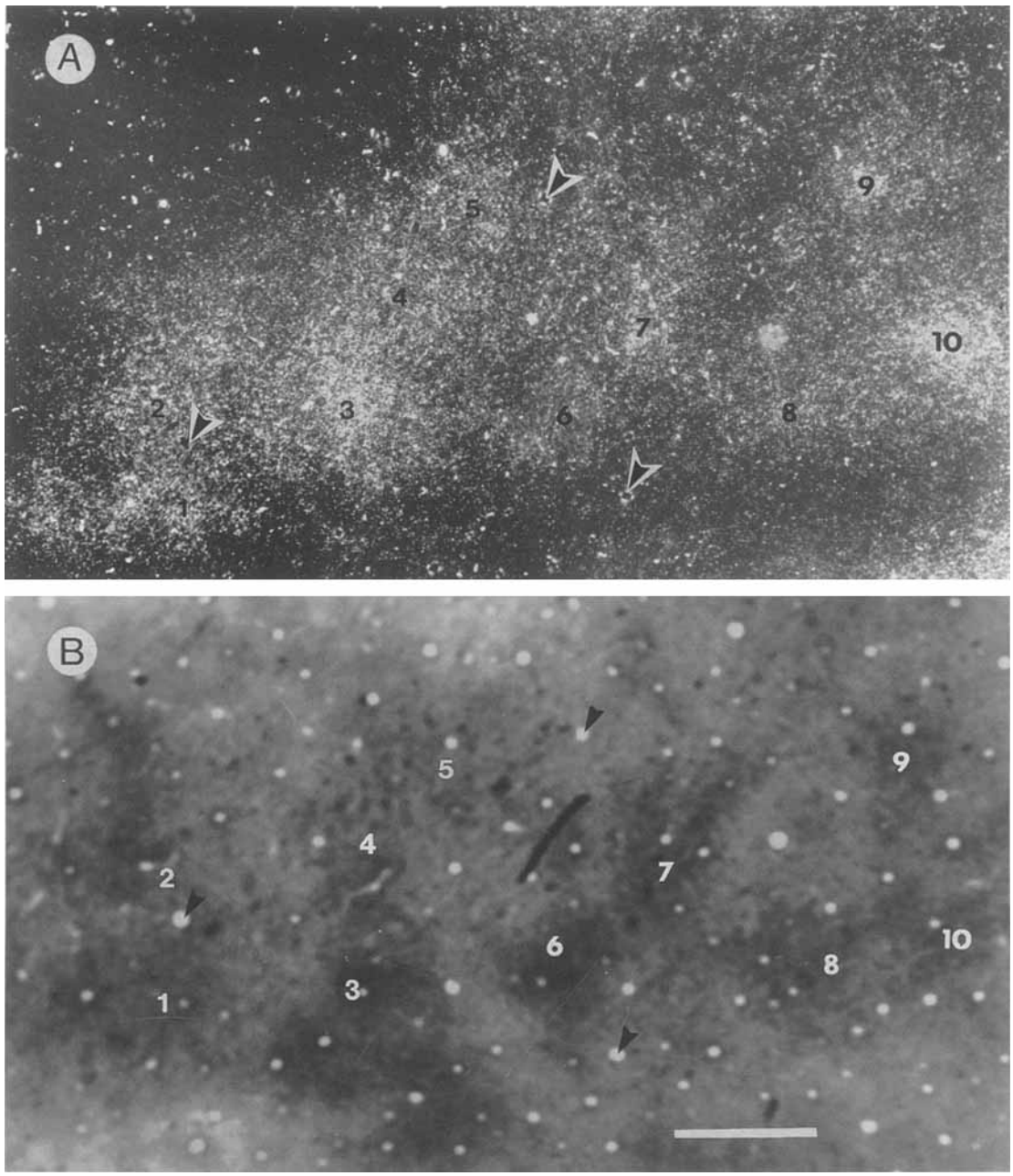

Fig. 14. Comparison of cytochrome oxidase blobs and C-laminae labeling in area 18. A: A tangential section through the lower part of layer 3 reacted for anterogradely transported WGA-HRP. **B:** A slightly deeper section reacted for cytochrome oxidase. Note that the correspondence between anterograde reaction product and CO blobs is present, albeit less robust than shown for area 17. Labeling conventions as in Figure 12. Scale bar, 1 mm, and applies to both A and B.

Relationship of C-laminae patches to ocular dominance columns

LeVay and Gilbert (1976) were the first to note that the projection from the C laminae to area 17 was patchy. They suggested that this patchiness was due to the fact that even though the C laminae receive inputs from both eyes, the input to the C laminae from the contralateral eye was greater than the input from the ipsilateral eye. It was thus suggested that the patches of C-laminae labeling represented the ocular dominance columns of the contralateral eye. In a similar vein, we have argued that the input from the C laminae to layer 4a is from Y-cells, and these Y-cells are thought to be confined to lamina C, which apparently receives input from the contralateral eye only. However, evidence from this study suggests that the C-laminae patches are not aligned solely with contralateral OD columns (Fig. 11). Moreover, it was shown in the present study that the patches of labeling from the C laminae align with the CO blobs, and the relationship of CO blobs and OD columns in the cat has been examined, albeit with slightly

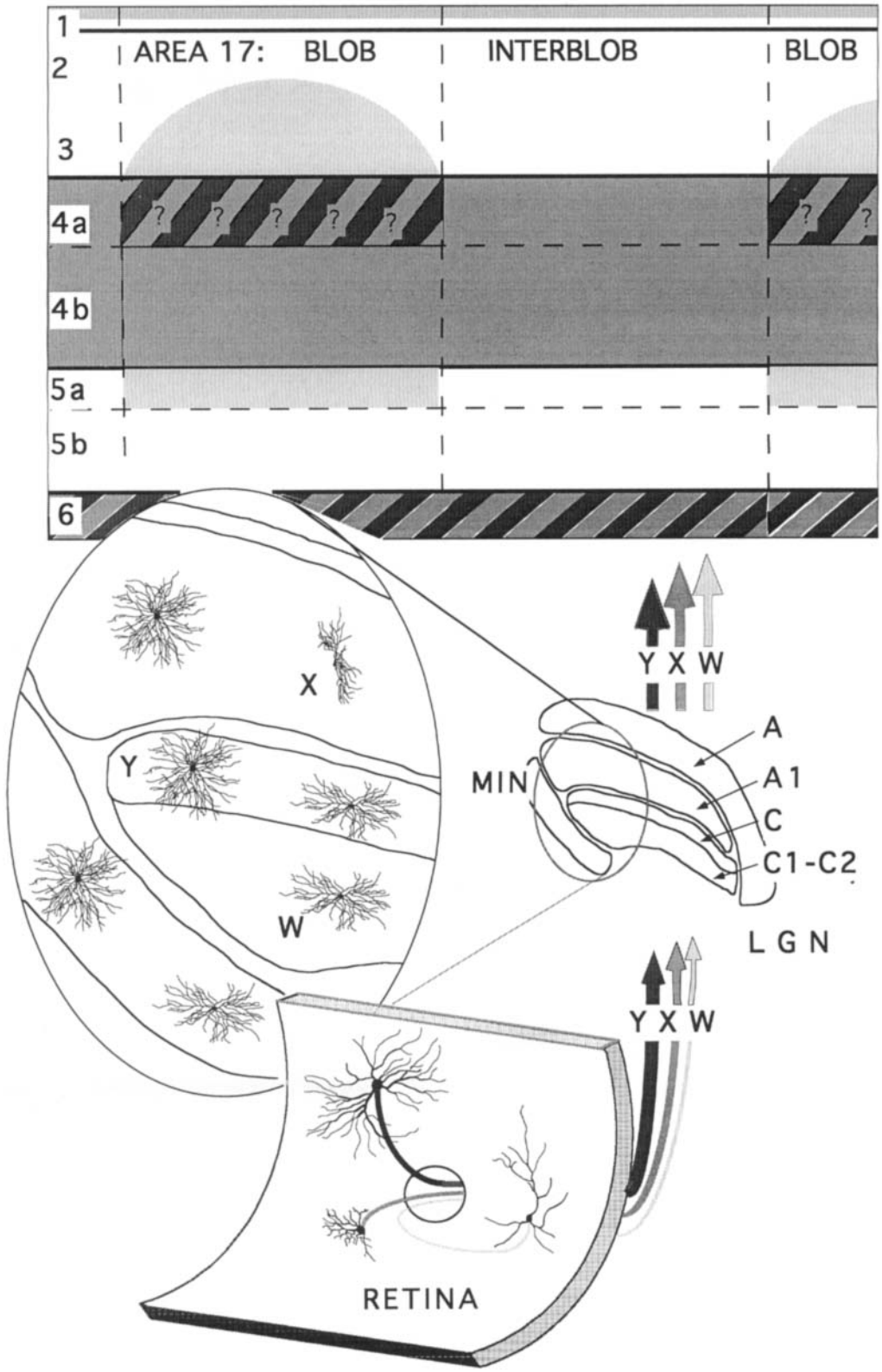

Fig. 15. Summary diagram of the X, Y, and W pathways of the cat's visual system. The diagram shows the three different cell classes in the retina (bottom), and the lateral geniculate (middle). The top part of the diagram shows the termination in area 17 of W-, X-, and Y-geniculocortical fibers, shown by three different densities of shading, W being lightest and Y being darkest. It is assumed that the Y-cell terminations from layer C described in this study are representative of all geniculate Y-cell terminations. The crosshatched pattern in layer 6 and layer 4a shows mixing of X-cell and Y-cell inputs. The X-cell input to layer 4a of the cytochrome oxidase blobs is marked with question marks because it was not possible to tell from this study whether X-cell terminations are found in or avoid the 4a blobs.

conflicting results (Murphy et al., 1991; Dyck and Cynader, 1993b). One study (Dyck and Cynader, 1993b) concluded that the OD and CO blob systems were independent, with CO blobs found roughly equally over both the centers and edges of OD columns, while the other study (Murphy et al., 1991) found that CO blobs tended to be associated with the centers of OD columns. Both of these studies, however, agree with this study in that CO blobs (and, hence, C-laminae labeling) in the cat were found over both contralateral and ipsilateral eye dominance columns. Thus, it is not likely that the patchiness of the C-laminae projections was due to OD columns.

If CO blobs are associated with both ipsilateral and contralateral OD columns, however, how can every CO blob, some of which must be over ipsilateral OD columns, have a Y-cell projection to layer 4a that apparently comes from the magnocellular lamina C, a contralateral eye-dominated layer? There are several possible explanations. First, cat OD columns are not as well defined as in macaque monkeys, for instance, and it has been argued that inputs from the contralateral eye are more confluent than those from the ipsilateral eye, which are more obviously patchy (Shatz et al., 1977). However, at least one recent study has shown that the segregation of inputs from the two eyes in the cat's visual cortex is better than previously expected (Hata and Stryker, 1994). Therefore, overlap of contralateral and ipsilateral inputs probably does not account for the Y-cell input into CO blobs over ipsilateral OD columns. Is it possible that an ipsilateral Y-cell-containing counterpart to the contralateral Y-cell-containing layer C exists? It has been noted that a few ipsilateral retinal Y-cell axons terminating in lamina A1 also send a collateral to the C-laminae (Bowling and Michael, 1984). Another, more likely source of ipsilateral Y-cell input to visual cortex is the large cells that are found in the intralaminar space between layers A1 and C. Often, the density of cells in this space is nearly as great as the density of cells in lamina C itself, making the border between lamina A1 and C much less clear than the border between lamina A and A1. The large size of cells in the intralaminar space is suggestive of Y-cells, and the position of these cells next to lamina A1 suggests that they could possibly receive ipsilateral inputs. Unpublished observations from this laboratory show that abundant retinal projections are made to the intralaminar space between A1 and C (but not between A and A1), although it is not yet known if they are from the ipsilateral or contralateral eye.

Geniculocortical projections in area 18

We also studied geniculocortical terminations in area 18. Previous studies have shown that X-cell input is lacking in area 18 (Tretter et al., 1975; Dreher et al., 1980; Harvey, 1980; Humphery et al., 1985b). The W-cell input in area 18 appears to have the same laminar termination pattern and relationship with the CO blobs as seen in area 17. The Y-cell input, however, has a different laminar pattern of termination in area 18 than in area 17. In agreement with the study of LeVay and Gilbert (1976), we found that labeling in layer 4 from the C laminae, instead of being confined to layer 4a as in area 17, extended throughout layer 4. However, labeling in layer 4 was often slightly patchy, being densest in the CO blobs, although the gaps between the patches were never as free of labeling as was the case in area 17. Sometimes the patchiness in layer 4 disappeared, showing complete filling-in with terminal labeling, although the W-cell terminations in layers 3 and 5a were still patchy. However, a similar pattern of layer 4 showing complete filling-in with patches of labeling in layer 3 and 5a was sometimes seen in area 17 following very large injections which spread to involve all layers of the geniculate at particular isoelevation representations; a similar explanation for the lack of patchiness in area 18 in some sections cannot be ruled out. Therefore, it is likely that projections from the C laminae are somewhat patchy in layer 4 of area 18. Projections from the A layers, however, appeared to be continuous in layer 4 of area 17, raising the possibility that projections from the C layers of the geniculate to area 18 are organized differently than projections from the A layers. However, both the A layer and the layer C projection to area 18 is thought to arise from Y-cells and, as discussed above, Y cells in the various parts of the LGN have not been shown to differ significantly.

Another explanation of these results is that Y-cell input from the different parts of the LGN to area 18 is similarly organized, but that input is not homogeneously distributed, being stronger to the blobs in layer 4a than to other parts of layer 4. Reconstructions of individual intracellularly filled Y-cell axons, from both A and C layers in area 18, have shown that, although these axons have projections to both layers 4a and 4b, the projection to layer 4a is invariably stronger than that to layer 4b (Freund et al., 1985). The patchiness of Y-cell axons, which we have suggested might be partly due to their selective termination in blobs, appears to be less distinct in area 18 than in area 17, with many more boutons distributed to the spaces between the patches (Humphery et al., 1985a,b). The single axon data are thus consistent with the hypothesis that the driving geniculate input that is responsible for the CO blobs of layer 4a of area 18 is the same, albeit more profuse, Y-cell input that is found in the other parts of layer 4. Presumably, when labeling of layer 4 in our experiments was relatively weak, the patchiness was visible; when the labeling, whether from A layers or C layers, was more robust, however, the patchiness was no longer visible due to the high contrast in the WGA-HRP reaction procedure. It would then be expected that a more quantitative labeling procedure would show a difference in numbers of Y-cell geniculate terminations between blobs and inter blobs in area 18. The increased CO activity in the layer 4a blobs of area 18 would thus be caused, not by the presence of a special class of inputs with higher activity than those that terminate elsewhere in layer 4, but by a higher concentration of the same inputs that terminate elsewhere in fewer numbers.

Comparisons with geniculocortical projections in other species

Finally, it is of interest to compare the segregation of geniculate terminations in the cat with those of other species. It appears that CO blobs in the cat, like those in primates, are associated with the segregation of different processing streams. The similarity between pathways in cats and primates is most striking for the comparison between the W-cell pathway of the cat and the so-called "koniocellular" pathway in primates. Like the parvicellular C layers of the cat, the koniocellular layers terminate in layer 3 selectively within the CO blobs (Fitzpatrick et al., 1983; Weber et al., 1983; Livingstone and Hubel, 1987b; Lachica and Casagrande, 1992) and, at least in galagos, contain cells with W-type physiological properties (Irvin et al., 1986). In tree shrews, geniculate input from small-cell

layers of the LGN also terminates specifically in layer 3 (Fitzpatrick and Raczkowski, 1990). (CO blobs have yet to be observed in this species.) One intriguing difference in the projections of the parvicellular C layers of the cat LGN and the small-cell layers in other species is the projection to layer 5a, which has only been described in the cat. Whether this pathway has analogs in other species is unknown.

In the cat, the CO blobs are visible in layer 4a, but not in layer 4b, and we have suggested that Y-cells in the C laminae may selectively target the CO blobs. It is interesting to note that, in the prosimian galago (Condo and Casagrande, 1990) and in the new world owl monkey (Horton, 1984), CO blobs are also visible in the top part of layer 4, similar to the arrangement of CO blobs in the cat. [This does not appear to be the case in other new world primates such as the squirrel monkey, or in any old world primates examined (Horton, 1984).] It has even been reported that the magnocellular inputs in the owl monkey are confined to the CO blobs in layer 4a (Horton, 1984), just as we suggest that Y-cell inputs from the C laminae are in the cat.

Another question concerning the similarity of geniculocortical organization in cats and primates is whether CO blobs in the cat are aligned with ocular dominance columns, as they are in most primates (Horton, 1984). At present, there are conflicting reports concerning this question (Murphy et al., 1991; Dyck and Cynader, 1993b). Certainly, the relationship between these two columnar systems cannot be as precise as it is in the macaque, for instance. This is because the spacing between CO blobs in the cat is too large to provide for blobs centered over the ocular dominance columns of each eye (compare Figs. 6A and 7A). In addition, ocular dominance columns in the cat have an irregular, highly branched pattern (Anderson et al., 1988). The relationship between CO blobs and ocular dominance does not hold for all primates, as evidenced by the squirrel monkey, in which inputs from the two eyes are nearly completely mixed, while CO blobs are very distinct (Weber et al., 1983; Horton, 1984). It may be that the variation in geniculocortical organization between primates and cats is not that much greater than the variation between different primate species (Debruyn et al., 1993).

It is concluded that CO blobs in cats and primates are manifestations of similar principles of geniculocortical organization. In both cats and primates CO blobs and inter blobs receive different combinations of geniculate inputs. We suspect that further study will show that other differences between blobs and interblobs in primates, such as intrinsic interlaminar connectivity (Lachica et al., 1992, 1993), dendritic field organization (Hübener and Bolz, 1992), and physiological response properties (Livingstone and Hubel, 1984; Tootell et al., 1988; Ts'o and Gilbert, 1988), will also be found between blobs and interblobs in the cat.

Note added in proof: A paper has come to our attention suggesting that the Y-cells in lamina C may represent a physiologically distinct group from those in lamina A and A1 based on contrast sensitivity functions (Frascella and Lehmkuhle, 1984).

ACKNOWLEDGMENTS

We thank Virginia Booth and Jin Zhang for technical assistance, and Bevil Conway for creating Figure 15. Gallamine triethiodide was a generous gift of Rhone-Poulenc Pharma. This study was supported by MRC Canada grant No. MT-9150 to JAM.

LITERATURE CITED

Anderson, P.A., J. Olavarria, and R.C. Van Sluyters (1988) The overall pattern of ocular dominance bands in cat visual cortex. J. Neurosci. *8:*2183–2200.

Berson, D.M. (1985) Cat lateral suprasylvian cortex: Y-cell inputs and corticotectal projection. J. Neurophysiol. *53:*544–556.

Bowling, D.B., and C.R. Michael (1980) Projection patterns of single physiologically characterized optic tract fibres in cat. Nature *286:*899–902.

Bowling, D.B., and C.R. Michael (1984) Terminal patterns of single, physiologically characterized optic tract fibres in the cat's lateral geniculate nucleus. J. Neurosci. *4:*198–216.

Boycott, B.B., and H. Wässle (1974) The morphological types of ganglion cells of the domestic cat's retina. J. Physiol. *240:*397–419.

Boyd, J., and J. Matsubara (1992) Segregated processing streams in cat visual cortex? Relationship of patchy connectivity to an extrastriate area, cytochrome oxidase staining, and local connections. Soc. Neurosci. Abstr. *18:*298.

Boyd, J.D., and J.A. Matsubara (1993) The C laminae of the cat lateral geniculate selectively target the cytochrome oxidase blobs. Soc. Neurosci. Abstr. *19:*298.

Bruce, L.L., and B.E. Stein (1988) Transient projections from the lateral geniculate to the posteriormedial lateral suprasylvian visual cortex in kittens. J. Comp. Neurol. *278:*287–302.

Bullier, J., and T.T. Norton (1979) Comparison of receptive field properties of X and Y ganglion cells with X and Y lateral geniculate cells in the cat. J. Neurophysiol. *42:*274–291.

Casagrande, V.A., and T.T. Norton (1991) Lateral geniculate nucleus: a review of its physiology and function. In A.G. Leventhal (ed): The Neural Basis of Visual Function. Houndmills, Basingstoke, Hampshire, and London, U.K.: The Macmillan Press, pp. 41–84.

Cleland, B.G., M.W. Dubin, and W.R. Levick (1971) Sustained and transient neurones in the cat's retina and lateral geniculate nucleus. J. Physiol. (Lond.), *217:*473–496.

Condo, G.C., and V.A. Casagrande (1990) Organization of cytochrome oxidase staining in the visual cortex of nocturnal primates (*Galago crassicaudatus* and *Galago senegalensis*). I. Adult patterns. J. Comp. Neurol. *293:*632–645.

Cresho, H.S., L.M. Rasco, G.H. Rose, and G.J. Condo (1992) Blob-like pattern of cytochrome oxidase staining in ferret visual cortex. Soc. Neurosci. Abst. *18:*298.

Crockett, D.P., S. Maslany, S.L. Harris, and M.D. Egger (1993) Enhanced cytochrome-oxidase staining of the cuneate nucleus in the rat reveals a modifiable somatotopic map. Brain Research *612:*41–55.

DeBruyn, E.J., V.A. Casagrande, P.D. Beck, and A.B. Bonds (1993) Visual resolution and sensitivity of single cells in the primary visual cortex (V1) of a nocturanal primate (bushbaby): Correlations with cortical layers and cytochrome oxidase patterns. J. Neurophysiol. *69:*3–18.

Dreher, B., A.G. Leventhal, and P.T. Hale (1980) Geniculate input to cat visual cortex: A comparison of area 19 with areas 17 and 18. J. Neurophysiol. *44:*804–826.

Dreher, B., and A.J. Sefton (1979) Properties of neurons In cat's dorsal lateral geniculate nucleus: A comparison between medial interlaminar and laminated parts of the nucleus. J. Comp. Neurol. *183:*47–64.

Dyck, R.H., and M.S. Cynader (1993a) Autoradiographic localization of serotonin receptor subtypes in cat visual cortex: Transient regional, laminar, and columnar distributions during postnatal development. J. Neurosci. *13:*4316–4338.

Dyck, R.H., and M.S. Cynader (1993b) An interdigitated columnar mosaic of cytochrome oxidase, zinc, and neurotransmitter-related molecules in cat and monkey visual cortex. Proc. Nat'l Acad. Sci. U.S.A. *90:*9066–9069.

Fitzpatrick, D., K. Itoh, and I.T. Diamond (1983) The laminar organization of the lateral geniculate body and the striate cortex in the squirrel monkey (*Saimiri sciureus*). J. Neurosci. *3:*673–702.

Fitzpatrick, D., and D. Raczkowski (1990) Innervation patterns of single physiologically identified geniculocortical axons in the striate cortex of the tree shrew. Proc. Natl Acad. Sci. U.S.A. *87:*449–453.

Frascella, J., and S. Lehmkuhle (1984) A comparison between Y-cells in A laminae and Lamina C of cat dorsal lateral geniculate nucleus. J. Neurophysiol. *52:*911–920.

Freund, T.F., K.A.C. Martin, P. Somogyi, and D. Whitteridge (1985) Innervation of cat visual areas 17 and 18 by physiologically identified X- and Y-type thalamic afferents. II. Identification of postsynaptic targets by GABA immunocytochemistry and Golgi Impregnation. J. Comp. Neurol. *242:*275–291.

Friedlander, M.J., and K.A.C. Martin (1989) Development of Y-axon innervation of cortical area 18 in the cat. J. Physiol. *416:*183–213.

Garey, L.J. (1971) A light and electron microscopic study of the visual cortex of the cat and monkey. Proc. R. Soc. Lond. B *179:*21–40.

Guillery, R.W. (1970) The laminar distribution of retinal fibers in the dorsal lateral geniculate nucleus of the cat: A new interpretation. J. Comp. Neurol. *138:*339–368.

Guillery, R.W., E.E. Geisert, E.H. Polley, and C.A. Mason (1980) An analysis of the retinal afferents to the cat's medial interlaminar nucleus and to its rostral thalamic extension, the "geniculate wing." J. Comp. Neurol. *194:*117–142.

Guillery, R.W., and M.D. Oberdorfer (1977) A study of fine and coarse retino-fugal axons terminating in the geniculate c laminae and in the medial interlaminar nucleus of the mink. J. Comp. Neur. *176:*515–526.

Harvey, A.R. (1980) The afferent connexions and laminar distribution of cells in area 18 of the cat. J. Physiol. *302:*483–505.

Hata, Y., and M.P. Stryker (1994) Control of thalamocortical afferent rearrangement by postsynaptic activity in developing visual cortex. Science *265:*1732–1735.

Hendrickson, A.E., J.R. Wilson, and M.P. Ogren (1978) Neuroanatomical organization of pathways between the dorsal lateral geniculate nucleus and visual cortex in old world and new world primates. J. Comp. Neurol. *182:*123–136.

Hickey, T.L., and R.W. Guillery (1974) An autoradiographic study of retinogeniculate pathways in the cat and the fox. J. Comp. Neurol. *1156:*239–254.

Hoffman, K.P., J. Stone, and S.M. Sherman (1972). Relay of receptive-field properties in dorsal lateral geniculate nucleus of the cat. J. Neurophysiol. *35:*518–531.

Horton, J.C. (1984) Cytochrome oxidase patches: A new cytoarchitectonic feature of monkey visual cortex. Phil. Trans. R. Soc. Lond. B *304:*199–253.

Horton, J.C., and D.H. Hubel (1981) Regular patchy distribution of cytochrome oxidase staining in primary visual cortex of macaque monkey. Nature *292:*762–764.

Hübener, M., and J. Bolz (1992) Relationships between dendritic morphology and cytochrome oxidase compartments in monkey striate cortex. J. Comp. Neurol. *324:*67–80.

Humphrey, A.L., M. Sur, D.J. Uhlrich, and S.M. Sherman (1985a) Projection patterns of individual X- and Y-cell axons from the lateral geniculate nucleus to cortical area 17 in the cat. J. Comp. Neurol *233:*159–189.

Humphrey, A.L., M. Sur, D.J. Uhlrich, and S.M. Sherman (1985b) Termination patterns of individual X- and Y-cell axons in the visual cortex of the cat: Projections to area 18, to the 17/18 border region, and to both areas 17 and 18. J. Comp. Neurol *233:*190–212.

Illing, R.-B., and H. Wässle (1981) The retinal projection to the thalamus in the cat: A quantitative investigation and a comparison with the retinotectal pathway. J. Comp. Neurol. *202:*265–285.

Irvin, G.E., T.T. Norton, M.A. Sesma, and V.A. Casagrande (1986) W-like response properties of interlaminar zone cells in the lateral geniculate nucleus of a primate (*Galago crassicaudatus*). Brain Res. *362:*254–270.

Kageyama, G.H., and M. Wong-Riley (1985) An analysis of the cellular localization of cytochrome oxidase in the lateral geniculate nucleus of the adult cat. J. Comp. Neurol. *242:*338–357.

Kageyama, G.H., and M. Wong-Riley (1986a) Laminar and cellular localization of cytochrome oxidase in the cat striate cortex. J. Comp. Neurol. *245:*137–159.

Kageyama, G.H., and M. Wong-Riley (1986b) The localization of cytochrome oxidase in the LGN and striate cortex of postnatal kittens. J. Comp. Neurol. *243:*182–194.

Lachica, E.A., P.D. Beck, and V.A. Casagrande (1992) Parallel pathways in Macaque Monkey striate cortex: Anatomically defined columns in layer III. Proc. Natl. Acad. Sci. U.S.A. *89:*3566–3570.

Lachica, E.A., P.D. Beck, and V.A. Casagrande (1993) Intrinsic connections of Layer-III of striate cortex in squirrel monkey and bush baby. Correlations with patterns of cytochrome oxidase. J. Comp. Neurol. *329:*163–187.

Lachica, E.A., and V.A. Casagrande (1992) Direct W-Like Geniculate Projections to the Cytochrome Oxidase (CO) Blobs in primate visual cortex-axon morphology. J. Comp. Neurol. *319:*141–158.

LeVay, S., and C.D. Gilbert (1976) Laminar patterns of geniculocortical projection in the cat. Brain Res. *113:*1–19.

Leventhal, A.G. (1979) Evidence that the different classes of relay cells of the cat's lateral geniculate nucleus terminate in different layers of the striate cortex. Exp. Brain Res. *37:*349–372.

Leventhal, A.G. (1982) Morphology and distribution of retinal ganglion cells projecting to different layers of the dorsal lateral geniculate nucleus in normal and Siamese cats. J. Neurosci. *2:*1024–1042.

Leventhal, A.G., R.W. Rodieck, and B. Dreher (1985) Central projections of cat retinal ganglion cells. J. Comp. Neurol. *237:*216–226.

Livingstone, M., and D. Hubel (1988) Segregation of form, colour, movement, and depth: Anatomy, physiology, and perception. Science *240:*740–749.

Livingstone, M.S., and D.H. Hubel (1983) Specificity of cortico-cortical connections in monkey visual system. Nature *304:*531–534.

Livingstone, M.S., and D.H. Hubel (1984) Anatomy and physiology of a color system in the primate visual cortex. J. Neurosci. *4:*309–356.

Livingstone, M.S., and D.H. Hubel (1987a) Connections between layer 4B of area 17 and the thick cytochrome oxidase stripes of area 18 in the squirrel monkey. J. Neurosci. *7:*3371–3377.

Livingstone, M.S., and D.H. Hubel (1987b) Thalamic inputs to cytochrome oxidase rich regions in monkey visual cortex. Proc. Natl. Acad. Sci. U.S.A. *79:*6098–6101.

Lorente de Nó, R. (1943) Cerebral cortex: Architecture, Intracortical Connections, Motor Projections. In J. Fulton (ed): Physiology of the Nervous System. Oxford: Oxford University Press, pp. 274–301.

Lund, J.S., G.H. Henry, C.L. MacQueen, and A.R. Harvey (1979) Anatomical organization of the primary visual cortex (area17) of the cat: A comparison with area 17 of the Macaque monkey. J. Comp. Neurol. *184:*599–618.

Mason, R. (1978) Functional organization in the cat's pulvinar complex. Exp. Brain Res. *31:*51–66.

Mesulam, M.M. (1978) Tetramethylbenzidine for horseradish peroxidase neurochemistry. J. Histochem. Cytochem. *26:*106–117.

Murphy, K.M., R.C. Van Sluyters, and D.G. Jones (1990) Cytochrome oxidase activity in cat visual cortex: Is it periodic? Soc. Neurosci. Abs. *16:*292.

Murphy, K.M., R.C. Van Sluyters, and D.G. Jones (1991) The organization of cytochrome oxidase blobs in the cat visual cortex. Soc. Neurosci. Abst. *17:*1088.

O'Leary, J.L. (1941) Structure of the area striata of the cat. J. Comp. Neurol. *75:*131–164.

Olavarria, J., and R.C. Van Sluyters (1985) Unfolding and flattening the cortex of gyrencephalic brains. J. Neurosci. Methods *15:*91–102.

Otsuka, R., and R. Hassler (1962) Über aufbau und gliederung der corticalen sehsphäre bei der katze. Archiv Psych. Z. Neurol. *203:*212–234.

Price, D.J. (1984) Patterns of cytochrome oxidase activity in areas 17, 18 and 19 of the visual cortex of cats and kittens. Exp. Brain Res. *159:*1–9.

Prusky, G.T., C. Shaw, and M.S. Cynader (1987) Nicotine receptors are located on lateral geniculate nucleus terminals in cat visual cortex. Brain Res. *412:*131–138.

Rauschecker, J.P., M.W. von Grünau, and C. Poulin (1987) Thalamo-cortical connections and their correlation with receptive field properties in the cat's lateral suprasylvian cortex. Exp. Brain Res. *67:*100–112.

Sanderson, K.J. (1971a) The projection of the visual field to the lateral geniculate and medial interlaminar nuclei in the cat. J. Comp. Neurol. *143:*101–118.

Sanderson, K.J. (1971b) Visual field projection columns and magnification factors in the lateral geniculate nucleus of the cat. Exp. Brain Res. *13:*159–177.

Shatz, C.J., S. Lindstrom, and T.N. Wiesel (1977) The distribution of afferents representing the right and left yes in the cat's visual cortex. Brain Research *131:*103–116.

Shipp, S., and S. Grant (1991) Organization of reciprocal connections between area 17 and the lateral suprasylvian area of cat visual cortex. Vis. NeuroSci. *6:*339–355.

Silverman, N.S., and R.B.H. Tootell (1987) Modified technique for cytochrome oxidase histochemistry: increased staining intensity and compatibility with 2-deoxyglucose autoradiography. J. Neurosci. Methods *19:*1–10.

Sur, M., M. Esguerra, P.E. Garraghty, M.F. Kritzer, and S.M. Sherman (1987) Morphology of physiologically identified retinogeniculate X- and Y-axons in the cat. J. Neurophysiol. *58:*1–32.

Tong, L. (1991) Development of the projections from the dorsal lateral geniculate nucleus to the lateral suprasylvian visual area of cortex in the cat. J. Comp. Neurol. *314:*526–533.

Tong, L., R.E. Kalil, and P.D. Spear (1982) Thalamic projections to visual areas of the middle suprasylvian sulcus in the cat. J. Comp. Neurol. *212:*103–117.

Tootell, R.B.H., M.S. Silverman, S.L. Hamilton, E. Switkes, and R.L. De Valois (1988) Functional anatomy of macaque striate cortex. V. Spatial frequency. J. Neurosci. *8:*1610–1624.

Tretter, F., M. Cynader, and W. Singer (1975) Cat parastriate cortex: A primary or secondary visual area? J. Neurophysiol. *38:*1099–1113.

Ts'o, D.Y., and C.D. Gilbert (1988) The organization of chromatic and spatial interactions in the primate striate cortex. J. Neurosci. *8:*1712–1727.

Tusa, R.J., L.A. Palmer, and A.C. Rosenquist (1978) The retinotopic organization of area 17 (striate cortex) in the cat. J. Comp. Neurol. *177:*213–236.

Tusa, R.J., A.C. Rosenquist, and L.A. Palmer (1979) Retinotopic organization of areas 18 and 19 in the cat. J. Comp. Neurol. *185:*657–678.

Weber, J.T., M.F. Huerta, J.H. Kaas, and J.K. Harting (1983) The projections of the lateral geniculate nucleus of the squirrel monkey: Studies of the interlaminar zones and the S layers. J. Comp. Neurol. *213:*113–145.

Wilson, P.D., M.H. Rowe, and J. Stone (1976) Properties of relay cells in the cat's lateral geniculate nucleus. A comparison of W-cells with X- and Y-cells. J. Neurophysiol. *39:*1193–1209.

Wong-Riley, M. (1979) Changes in the visual system of monocularly sutured or enucleated cats demonstrable with cytochrome oxidase histochemistry. Brain Res. *171:*11–28.

Wong-Riley, M., and D.A. Riley (1983) The effect of impulse blockage on cytochrome oxidase activity in the cat visual system. Brain Research *261:*185–193.

Wong-Riley, M.T.T., S.C. Tripathi, T.C. Trusk, and D.A. Hoppe (1989) Effect of retinal impulse blockage on cytochrome oxidase-rich zones in the macaque striate cortex. I. Quantitative electron-microscopic (EM) analysis of neurons. Visual Neurosci. *2:*483–497.